A thesis for the Degree of Doctor of Philosophy

Smoking Effects on Cyclic Variation in Blood Echogenicity from Carotid Artery

Ying Li

Oceanic Information and System Engineering

GRADUATE SCHOOL

JEJU NATIONAL UNIVERSITY

2011. 2

Smoking Effects on Cyclic Variation in Blood Echogenicity from Carotid Artery

Ying Li

(Supervised by Professor Dong-Guk Paeng)

A thesis submitted in partial fulfillment of the requirement
for the degree of Doctor of Philosophy

2011. 02.

This thesis has been examined and approved.

이 종 헌
Chair of committee, Chong Hyun Lee, Prof. of Department of Ocean System Engineering

최 민 주
Min Joo Choi, Prof. of Department of Medicine

배 진 호
Jinho Bae, Prof. of Department of Ocean System Engineering

최 재 철
Jay Chol Choi, Prof. of Department of Medicine

Paeng
Dong Guk Paeng, Prof. of Department of Ocean System Engineering

2010. 12
Date

Oceanic Information and System Engineering
GRADUATE SCHOOL
JEJU NATIONAL UNIVERSITY

谨献于

Dedicated to

母亲陆廷霞和未婚妻苏秀真

Ting Xia Lu and Ellen Sovian

ACKOWLEDGEMENTS

Ph.D. studies in Jeju National University are a valuable experience in my life. Jeju became my second hometown. It is truly a world outside garden, wherein the simple life clarified my aspiration in research. I would like to thank my supervisor, Professor Dong Guk Paeng, for enabling me to undertake these studies, for giving me guidance as a wonderful adviser in research, for caring me like a loving mother, for joking with me like a close brother, for blaming me like a rigorous father, and for letting me know our heavenly father. I will never regret being a disciple of Professor Dong Guk Paeng. I would like to thank Professor Jinho Bae and Professor Chong Hyun Lee. Their classes have proven to be one of my best learning experiences at Jeju National University. In their weekly meetings, I always got the first comment from them in each step of my research. They are the most thorough reviewers. I would also like to thank Professor Min Joo Choi. He is like my other supervisor, always giving suggestions and support for my research. This research can hardly be finished without his help. I would like to offer special thanks to Professor Jay Chol Choi, who has given a lot helpful suggestions and valuable samples in the initial stage of this study. I would like to express my sincerest gratitude to Professor Il Hyoung Cho and Professor Joon Young Kim for their encouragement and assistance in the duration of my course work.

I have been fortunate enough to have the support of so many people in the research group. Without them this thesis would not have been possible - Jeong Hwa Yang, Hyeok Jun Koh, Tae Hoon Bok, Gwan Suk Kang, S.R.Anjaneya reddy, Seung Woo Byun, Jea Il Lee, Juho Kim, and

Sung Hyub Ko. Special thanks are given to my two co-workers, Tae Hoon Bok and Jeong Hwa Yang. We had spent many days and nights working on projects. Our spirit of cooperation is truly commendable. Gwan Suk Kang and Tae Hoon Bok are friends whom I can always bother, and problems solvers for me all the time. My life in Korea was not troubled as an alien because of them. I hereby extend my hearty thanks to both of them. I would also like to thank those foreign friends who gave me a lot of help. Most of them already left Korea, in particular-Umer Zee shan Ijaz, Xiao Rui, Wang Ning, Farrukh Aslam Khan, Pham Minh Anh, Shafqatur-rehman, Mano Samuel Andrews and Chen Huan. I gratefully acknowledge financial support from the National Research Foundation Grant funded by the Korean Government. I greatly appreciate the participation of all the volunteers in this study. All of them are university students or teachers in Jeju National University and Cheju Halla College, who are from Sri Lanka (2), Bengal (2), India (4), Pakistani (5), Korea (28), and China (32).

I would also like to thank my family who has been extremely understanding and supportive of my studies. I feel very lucky to have Ellen Sovian as my fiancée, who can bear with me when I was too busy with my work. Her love is always my source of strength. Finally, I would like to thank my mother, Ting Xia Lu, for taking care of me in the later part of my Ph.D. studies, and for giving me the motivation to finish this thesis.

ABBREVIATIONS AND NOTATIONS

A_{cve}	Amplitude of cyclic variation in echogenicity
A'_{cve}	Compensated A_{cve}
AE	Average echogenicity
BMI	Body mass index
BP	Blood pressure
BPM	Beat per minute
CC	Carboxyhemoglobin concentrations
CVE	Cyclic variation in echogenicity
DCC	Daily consumption of cigarettes
EDTA	Ethylenediaminetetraacetic acid
EDV	End diastolic velocity
FC	Fibrinogen concentration
H	Hematocrit
HF	Hough transform
HR	Heart rate
i.d.	Inner diameter
M	RBC aggregation index at high shear rate
M1	RBC aggregation index at low shear rate
M_{cve}	Minimum echogenicity in a cycle

M'_{cve}	Compensated M_{cve}
o.d.	Outer diameter
PSV	Peak systolic velocity
RBC	Red blood cell
RBCF	Red blood cell filtration
RBCA	Red blood cell aggregation
SNR	Signal to noise ratio
SY	Smoking year
PV	Plasma viscosity
WBV	Whole blood viscosity
WEH	Weekly exercise hours

CONTENTS

LIST OF FIGURES

LIST OF TABLES

SUMMARY

The dynamic changes of echogenicity in common carotid artery was first observed from coded harmonic images by LOGIQ 700 Expert GE ultrasound system (GE, Milwaukee, WI, USA) by Paeng et al [1]. The observed variation in echogenicty was related with the dynamic change of red blood cell (RBC) aggregate during a cardiac cycle. Coded harmonic image was suggested as a better means in characterizing RBC aggregation [1]. In this research, the cyclic variation in echogenicity (CVE) was observed in the transverse section of the common carotid artery through another commercialized ultrasound system (Voluson e, GE). In order to confirm that the increased harmonic echogenicity is mainly from RBC aggregation, the harmonic images from porcine whole blood and RBC suspension were measured as a function of flow speed under steady flow in a mock flow loop. Harmonic echogenicity from porcine whole blood decreased exponentially with flow speed at lower speed while the one from RBC suspension did not vary with flow speed. These are in agreement with previous results from another ultrasound system of GE LOGIQ 700 Expert [1]. Thus, shear rate dependent RBC aggregation is a determining factor in dynamic changes of echogenicity, and validates that the coded harmonic echogenicity measured from this commercialized ultrasound system reflects the variation of RBC aggregation *in vivo*.

To better understand this observed CVE, the amplitude of CVE (A_{cve}) was analyzed among 28 smokers before and after smoking. Smoking has acute effects on A_{cve} and acute changes in A_{cve} induced by smoking are different between heavy smokers and light smokers.

The increase in A_{cve} after smoking was significantly higher in the heavy smokers (4.98±4.26) compared with light smokers (-0.3±3.01). Moreover, A_{cve} and minimum echogenicity in a cycle (M_{cve}) were compared among 17 nonsmokers, 11 light smokers, and 17 heavy smokers. The effects of tissue attenuation on A_{cve} and M_{cve} were compensated with body mass index (BMI). Compensated A_{cve} is significantly higher in heavy smokers (36.7±9.5) and light smokers (35.2±5.1) compared with nonsmokers (29.3±7.9; $P<0.05$). However, there is no significant difference for compensated M_{cve} among three groups.

This study is the first measurement and analysis of *in vivo* change of CVE in blood due to smoking using harmonic images collected by a GE Voluson e ultrasound system. The effects of smoking on CVE were discussed with hemodynamic and hematological changes caused by smoking. The change of CVE induced by smoking was suggested as a reflection of the change of RBC aggregation tendency. The potential of A'_{cve} to estimate RBC aggregation *in vivo* was also presented in this thesis.

Chapter 1

INTRODUCTION

1.1 Background

Red blood cell (RBC) aggregation is a phenomenon wherein the RBCs stick together to form rouleaux (left panel of Fig.1.1) at lower shear rates and break up at higher shear rate. It is a dynamic and reversible process in flowing blood. With increased RBC aggregation, blood viscosity increases and local blood flow decreases. RBC aggregation has a direct effect on the formation of thrombus at low shear rates [2] and may create problems at the level of microcirculation [3]. Elevated RBC aggregation is considered as an independent risk factor for vascular occlusive disorder [4-5] and thrombus [3-6]. However, the mechanisms of RBC aggregation are not yet fully understood. Most techniques for measuring RBC aggregation are only applicable under *in vitro* conditions. Several studies have shown that ultrasound backscattering power from blood was highly related to the state of RBC aggregation, therefore suggesting as a potential tool in monitoring RBC aggregation *in vivo* [7-10]. However, RBC aggregation *in vivo* is only observed in a few studies. The cyclic variations in echogenicity (CVE) was first observed as coded harmonic images of healthy common carotid arteries by Paeng et al. [11]. The origin of this observed CVE was studied in an *in vitro* experiment [1]. This observed CVE was suggested to be related with the dynamic change of RBC aggregation *in vivo*. However, no proof from *in vivo* experiment to support this

suggestion has been found.

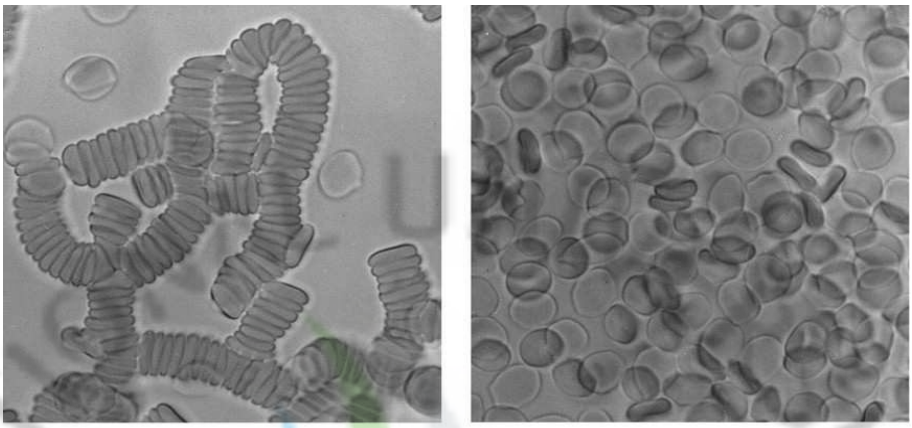

Fig. 1.1. Photomicrographs of human RBCs in plasma (left panel) and in saline (right panel). Magnification × 400 [12]

Smoking is the single largest preventable cause of diseases and premature death [13]. The number of deaths annually attributable to smoking is 3 million in the world in 1993 and is expected to increase to 8.4 million in 2020 [14]. Smoking is responsible to more than a quarter of all deaths from heart diseases and about three-quarters of the world's chronic bronchitis. Smoking has been increasingly recognized to be related with vascular disease. Its mechanism in causing vascular disease is still not very clear. Therefore, the smoking effects on hematologic and hemodynamic parameters are an important topic and a lot of experiments have already been performed. Acute and chronic smoking effects on hematological and hemodynamic parameters are summarized in Table 1.1. The parameters related with RBC aggregation are discussed blow.

Chronic smoking effects on hematologic and hemodynamic parameters

Several blood parameters were frequently found to be elevated in smoking group compared with a nonsmoking group, such as plasma viscosity [15-17], whole viscosity [16-17], hematocrit [17-19], fibrinogen concentrations [16-17, 19-22], and RBC aggregation [17-18, 23], e.g., M (RBC aggregation rate at high shear rate in Fig. 1.2) , and M1 (RBC aggregation rate at low shear rate in Fig. 1.3) significantly increased from the nonsmokers to the light and heavy smokers.

Additionally, blood pressure (BP) is significantly higher in male and female smokers compared with nonsmokers. However, the smoking effect on heart rate is only statistically significant for male smokers, but not for female smokers [24]. Increased HR and BP would influence blood flow, and subsequently affect RBC aggregation. Hence, chronic cigarette smoking could affect RBC aggregation by changing both blood constituents and blood flow properties.

Acute smoking effects on hematologic and hemodynamic parameters

Smoking chronic effects on many hematological parameters are well documented. However, the acute response of most hematological parameters to smoking appears to be unexplored. Fibrinogen concentrations [16] and hematocrit [16, 25-26] were significantly decreased after smokers stopped smoking for several days. No report about the acute response of RBC aggregation and whole blood viscosity to smoking can be found. The forearm vascular

resistance [27] and calf vascular resistance [28] increased during smoking. This increased vascular resistance possibly reflects the increase in RBC aggregation and blood viscosity. In contrast, a significant reduction in red cell filtration has been reported after smoking of two or three cigarettes for smokers [29-30] and one cigarette for nonsmokers [31]. Thus, acute smoking could decrease RBC deformation. Several studies have clearly indicated that effective aggregation requires large areas of intimate membrane contact between cells and decreased deformability may decrease RBC aggregation [32-33]. Therefore, further investigation on the acute effects of smoking on RBC aggregation is needed.

On the other hand, HR increases after smoking. After smoking 1 cigarette, HR of subjects increased 5–10 BPM, and was restored after 90 min when no more nicotine was consumed [34-35]. The increase in HR after smoking is dependent on the dose [36-37] and subject-specific factors such as age [38], gender [39-41], blood type [42], hostility [43], and circadian typology [44]. Furthermore, the systolic and diastolic blood pressure increased during smoking [27-28] and after smoking [45], in agreement with the report that HR increases with both systolic and diastolic blood pressure [46]. Therefore, smoking could acutely affect RBC aggregation through its influence on hemodynamic parameters, even though the acute effects of smoking on hematological parameter are unknown.

Smoking has significant chronic and acute effects on the RBC aggregation. Therefore, acute smoking effects on CVE are required to study and it may provide useful information for better monitoring RBC aggregation using ultrasound techniques *in vivo*.

Table 1.1. Acute and chronic smoking effects on hematological parameters

	Acute smoking effects	Chronic smoking effects
WBV	Galea et al. 1985	Ernst et al. 1987
PV	Galea et al. 1985	Ernst et al. 1987
FC	Galea et al. 1985	Ernst et al. 1987; Pilgeram et al.1968, Shasha et al. 1993
H	Galea et al. 1985 Bain et al, 1992	Ernst et al. 1987; Tollerud et al.1989, Shasha et al. 1993
CC	Lagrue et al. 1979 Lowe et al.1980	Ernst et al. 1987
RBCF	Lagrue et al. 1979 Lowe et al.1980	Dintenfass, 1975; Boss et al, 1973; Demiroglu et al. 1997
RBCA	None	Arronow, 1976; Astrup et al, 1967; Garrison et al, 1978
BP	Houben et al. 1981 Grassi et al. 1994	Al-Safi 2005
HR	Benowitz 1988 Hayano et al. 1990	Al-Safi 2005

WBV=Whole blood viscosity; PV= Plasma viscosity; FC= Fibrinogen concentrations; H=Hematocrit; CC= Carboxyhemoglobin concentrations; RBCF=Red blood cell filtration; RBCA=red blood cell aggregation; BP=Blood pressure; HR=Heart rate.

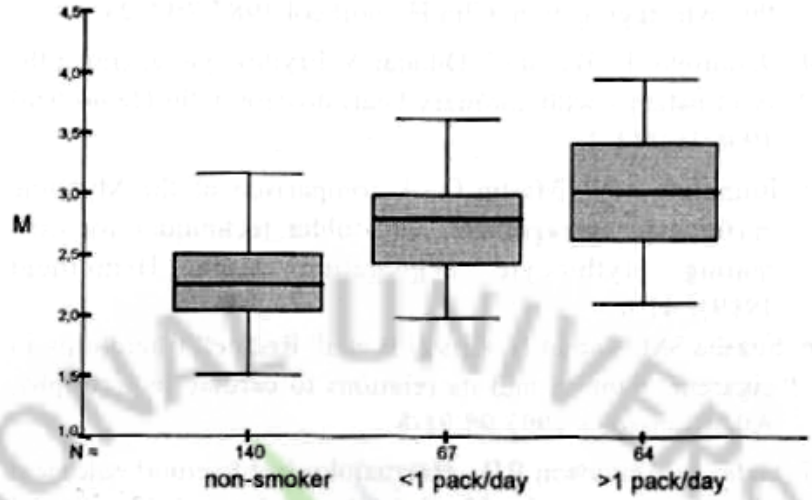

Fig. 1.2. Effect of smoking on RBC aggregation at high shear rate (M=RBC aggregation index at high shear rate) [18].

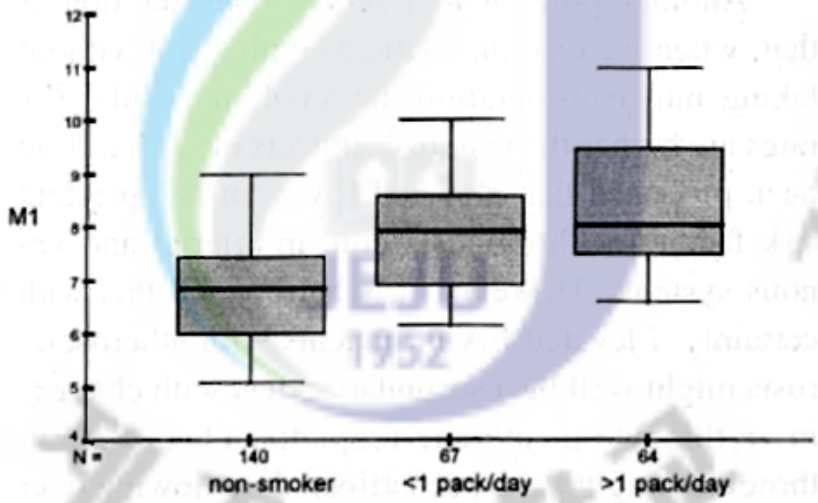

Fig. 1.3. Effect of smoking on RBC aggregation at low shear rate (M1=RBC aggregation index at low shear rate) [18].

1.2 Previous studies

Several research groups have shown that ultrasound backscattering from blood depends on RBC aggregation *in vitro* [7-10]. Another group has demonstrated that backscatter is significantly higher in veins than in the arteries and significantly higher in patients with hyperlipidemia than in normal individuals *in vivo* [47].

Under pulsatile flow, the ultrasound backscattering power and, consequently, the echogenicity of blood vary cyclically due to the dynamic changes of RBC aggregation in flowing blood. De Kroon et al. [48] was the first to demonstrate CVE *in vivo*. Shortly after, the cyclic variations in Doppler backscattering power was also measured *in vitro* using porcine blood [49]. However, the cyclic variations in Doppler power are only apparent at 20 beats per minute (BPM), not at 70 BPM [49-50]. Subsequent studies have demonstrated that cyclic variations in Doppler power are dependent on stroke rate, i.e., more evident at low stroke rates [51-54]. Recently, variations in echogenicity of porcine blood have been observed at 70 BPM with a high-frequency (35 MHz) transducer using a Couette flow system [55]. Furthermore, Huang [56] found that the cyclic variations in integrated backscatter of porcine blood are more easily recognized using a high-frequency transducer at lower peak flow velocities and fixed stroke rates. Thus, cyclic variations in echogenicity and backscattering power are not obvious at high stroke rates or high peak flow velocities, requiring transducers with higher frequencies and better sensitivities.

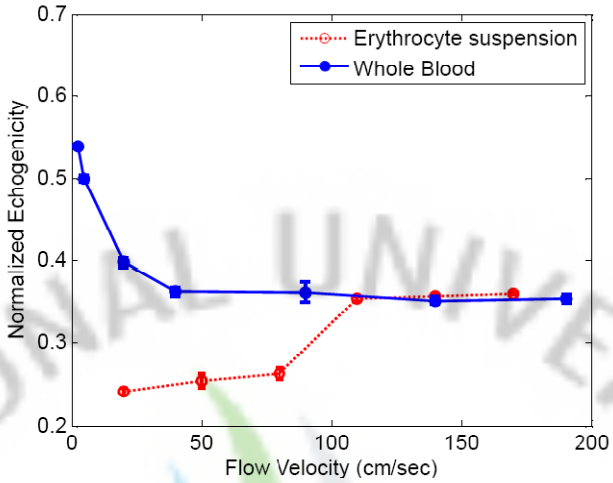

Fig.1.4. Harmonic echogenicity from porcine whole blood and erythrocyte suspension as a function of flow velocity, the echogenicity, and flow velocity were taken from the tub center under steady flow. Results are mean ± standard deviation of six snapshots [1].

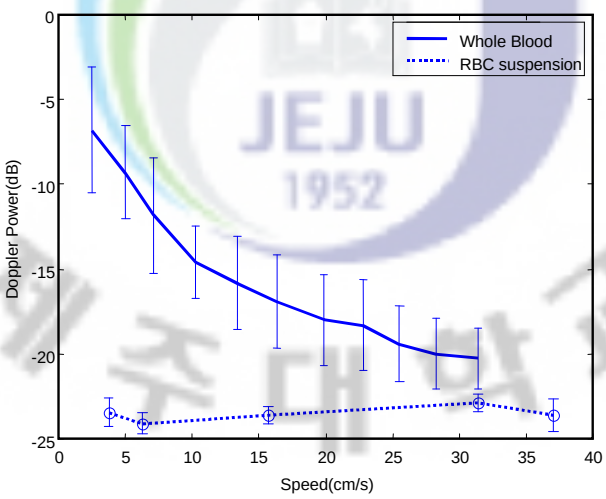

Fig.1.5. The Doppler power from porcine whole blood and red blood cell (RBC) suspensions under steady flow. The solid line is for whole blood and the dotted line is for RBC suspensions. These results represent the averages from 3 different porcine blood samples. Standard deviations are shown as error bars. Hematocrit of whole blood and RBC suspensions is 20%. [53].

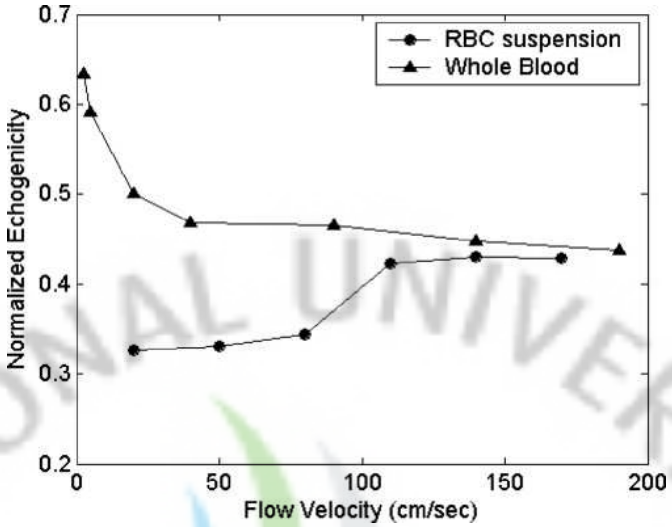

Fig.1.6. The echogenicity variation from whole blood and RBC suspension as a function of flow velocity. The echogenicity and flow velocity were taken from the tube center under steady flow [57].

The cyclic variation in echogenicity was first observed *in vivo* from coded harmonic images of healthy carotid arteries by Paeng et al [11] using a GE LOGIQ 700 Expert system (GE, Milwaukee, WI, USA). This is the only noninvasive *in vivo* observation of CVEs in common carotid artery. The smoke-like echogenicity from blood can easily be connected with the artifact, which is often appears in B-mode imaging. To ensure that the observed cyclic variation in echogenicity truly reflects the backscattered power from RBC and the dynamic change of RBC aggregation, the harmonic echogenicity from porcine blood and RBC suspension were measured as a function of flow speed. The echogenicity from whole blood decreased with increase in flow velocity and constant at higher velocities. The echogenicity of RBC suspension, in contrast, was found to be lower and did not vary with the flow velocity, except for the increase at velocities greater than 100cm/s, which might be attributed to the

presence of flow disturbances (Fig.1.4). These results were in agreement with the previous *in vitro* finding from the Doppler power (Fig.1.5) and B-mode imaging (Fig.1.6), indicating that erythrocyte aggregation is shear rate dependent, validating harmonic imaging as a means for measuring erythrocyte aggregation.

1.3 Specific Aims

In this study, the variation in echogenicity from common carotid artery was observed using another ultrasound system (GE Voluson e). This research aims to provide both *in vitro* and *in vivo* evidences to affirm the origin of observed CVE, suggesting its potential in practical applications. We have been working to achieve this goal as followings.

To ensure the collected echogenicity using GE Voluson e reflect the backscattered power from RBC, and present the dynamical change of RBC aggregation, the harmonic echogenicity from porcine blood and RBC suspension was measured as a function of flow speed.

To better evaluate the CVE, a Matlab code was developed to automatically identify the arterial wall in the cross sectional image of the carotid artery. The echogenicity from the central region of the artery was recorded in time sequence. An index was used to describe the amplitude of CVE, namely A_{cve}.

To explore the relationship among smoking, CVE, and RBC aggregation, A_{cve} was measured and compared before and after smoking and between smokers and nonsmokers.

1.4 Thesis Outline

Chapter 2 provides relevant background knowledge for this study such as the blood properties, ultrasonic scattering theories and harmonic imaging.

Chapter 3 presents experimental results of harmonic echogenicity from aggregating porcine whole blood and non-aggregating RBC suspensions as a function of flow speed under steady flow in a mock flow loop. This experiment aims to investigate the origin of the variation in blood echogenicity measured by GE Voluson e ultrasound system. The same ultrasound system with the same probe setup was used for the *in vivo* experiment.

Chapter 4 describes the method in identifying the boundary of blood vessel with Hough transform and calculates the amplitude index of CVE. The potential and limitation of this amplitude index was also discussed.

Chapter 5 reports the acute smoking effects on A_{cve} from an experiment involving 28 smokers. The change of A_{cve} before and after smoking was studied in the heavy smoker group and light smoker group. The possible acute smoking effects on hematological parameters were suggested.

Chapter 6 suggests a method in compensating the effect of tissue attenuation on A_{cve}, and the compensated A_{cve} was compared among non-smoker group, light smoker group, and heavy smokers group. The compensation method of A_{cve} was discussed.

Chapter 7 summarizes the findings in this research, and suggests future studies.

Chapter 2

BACKGROUND KNOWLEDGE

2.1 Blood properties

Blood is a living tissue that circulates through the heart, arteries, veins, and capillaries carrying nourishment, electrolytes, hormones, vitamins, antibodies, heat, and oxygen to the body's tissues. It contains red blood cells, white blood cells, and platelets suspended in a fluid base called plasma. Plasma is a Newtonian viscous fluid whose viscosity is about 1.2 cP, but whole blood behaves like a non-Newtonian fluid whose viscosity varies with hematocrit, the protein concentration of the plasma, the deformability of the blood cells, and the tendency of the blood cells to aggregate [58]. The shape of human RBC is a biconcave disc with a diameter of approximately 8.2 μm and thickness about 2.2 μm. Red blood cells (RBC) are the main component of blood (45% of total blood volume). They are much more numerous than the white blood cells ($1/600^{th}$ of cellular volume) and platelets ($1/800^{th}$ of cellular volume). Therefore, the backscattering of ultrasound by blood was considered almost entirely due to the RBC [58].

2.2 Ultrasonic scattering from blood

The ultrasound backscattered power from RBCs is dependent on their size, concentration, and acoustic properties. When an ultrasonic wave encounter a particle that is very small in size

compared to the incident wavelength, a part of the incident energy is uniformly scattered in all directions. This kind of wave scattering was first studied by Lord Rayleigh in 1871 and is therefore referred to as Rayleigh scattering.

Rayleigh scattering occurs over frequency range 2 to 60 MH, when an RBC is a scattering target [9]. By assuming Rayleigh scattering, a spherically shaped RBC, and an observation point many wavelengths distant from the scatter, the scattering cross section is obtained as [59]:

$$\sigma(\phi) = \frac{\pi^2 f^4 V_e^2}{c_0^4}\left[\frac{\kappa_e - \kappa_0}{\kappa_0} - \frac{\rho_e - \rho_0}{\rho_e}\cos\phi\right]^2 \tag{2.1}$$

where V_e is the volume of a red blood cell, f is the frequency of the transmitted ultrasonic wave, c_o is the speed of sound in blood, ϕ is the angular direction of the scattered signal relative to the direction of the transmitted beam, k and ρ are, respectively, the compressibility and mass density, and the subscripts *e* and *o* represent the red blood cell and the ambient fluid media, respectively.

The scattering cross-sectional area is defined as the power scattered by one spherical particle per unit incident intensity per unit solid angle in a direction ϕ with respect to the ultrasound beam. It is a very important parameter used to define the ultrasound backscattering properties [59]. Since the intrinsic properties of red blood cells and the speed of sound in the media do not vary much, the backscattering cross section is mainly dependent on the volume of a red blood cell, and frequency. Rayleigh scattering predicts that the backscattered power

from one particle is proportional to the square of the particle volume and the fourth power of frequency. Therefore, rouleaux formation in whole blood may significantly affect the backscattered power at a fixed frequency.

2.3 Modeling of ultrasonic scattering from blood

The RBCs are so densely packed in normal human blood that they interact strongly and cannot be treated as independent scatterers. Two stochastic models were first proposed to simulate the density and compressibility function of the packed RBCs at high hematocrit blood, which is a random medium. The particle model used the backscattered wavelets from an individual RBC, and the continuum model used the density and compressibility fluctuation of the medium as source terms. These two models were later integrated in the hybrid model [60].

Mo and Cobbold (1986) [61] proposed a general particle scattering model assuming blood as a suspension of RBC aggregates and that all scatterers in the blood sample have RBCs of identical size. The backscattering coefficient (BSC) is given by

$$BSC = \sigma_{bs} \frac{H}{V_e} W \qquad (2.2)$$

where σ_{bs} is the backscattering cross-section obtained for Eq. 2.1 for $\phi=180^{o}$, W is a packing factor which is a measure of the correlation amongst scatterers.

In the continuum model, *BSC* is defined by the following expression, assuming scattering

is considered to arise from spatial fluctuations in the density and compressibility of the continuum,

$$BSC = \overline{\sigma_{bs}} \frac{\overline{\mathrm{var}(n)}}{\Omega_0} \tag{2.3}$$

where Ω_0 is an elemental blood volume known as a voxel, $\overline{\sigma_{bs}}$ is the average backscattering cross section in the random medium, and $\overline{\mathrm{var}(n)}$ is the variance in the number of scatterers in Ω_0 obtained by averaging over space and time.

The two models were integrated in the hybrid model by Mo and Cobbold (1992) [60], who combined the influence of the mean number of scatterers per voxel and its variation in number as a function of time. BSC in this hybrid model is given as

$$BSC = \sigma_{bs} \frac{\overline{\mathrm{var}(n)}}{\Omega_0} = \sigma_{bs} \frac{\bar{n}}{\Omega_0} W \tag{2.4}$$

where $\bar{n}$ is the mean number of scatterers in the voxels Ω_0, W is a packing factor.

2.4 Harmonic imaging

The region of blood flow in B-mode images is normally displayed as a uniform black zone and no variation in echogenicity from the vessel lumen is observed because the signal from blood is much weaker than that from tissue. However, cyclic variation in echogenicity from human carotid artery was observed in the coded harmonic imaging collected by a GE LOGIQ 700 system with an M12L probe. And coded harmonic imaging was suggested as a

good tool to study backscattering from human blood *in vivo* [1]. The basic processing of three harmonic imaging technologies was summarized by Lee et al. [62]

Coded harmonic imaging was based on GE's proprietary digitally encoded ultrasound technology. This technology uses coded pulse sequences, which is obtained by repeating and amplitude-modulating the base unit according to a digital code, and is comprised of (±) 1s and 0s only. When a code applies to the transmitter pulse sequence, the receive decoder could recognize fundamental frequency brand, and then remove it without affecting the second harmonic frequency band.

Pulse inversion harmonic imaging was implemented by transmitting two identical pulses with reverse polarity to the medium and adding the two resultant returned signals cancels the fundamental linear components and preserves the nonlinear harmonic components. Because no filtering technique is used, the wideband information is preserved.

Conventional tissue harmonic imaging applied a frequency domain filter to remove the fundamental frequency band that contains reverberation and other acoustic noises. Due to overlap between the fundamental and second harmonic frequency band, the filtering approach always tends to remove a significant portion of the second harmonic frequency band. Thus, even although the transmit signal is wideband, the result is a narrowband harmonic signal and reduced axial resolution.

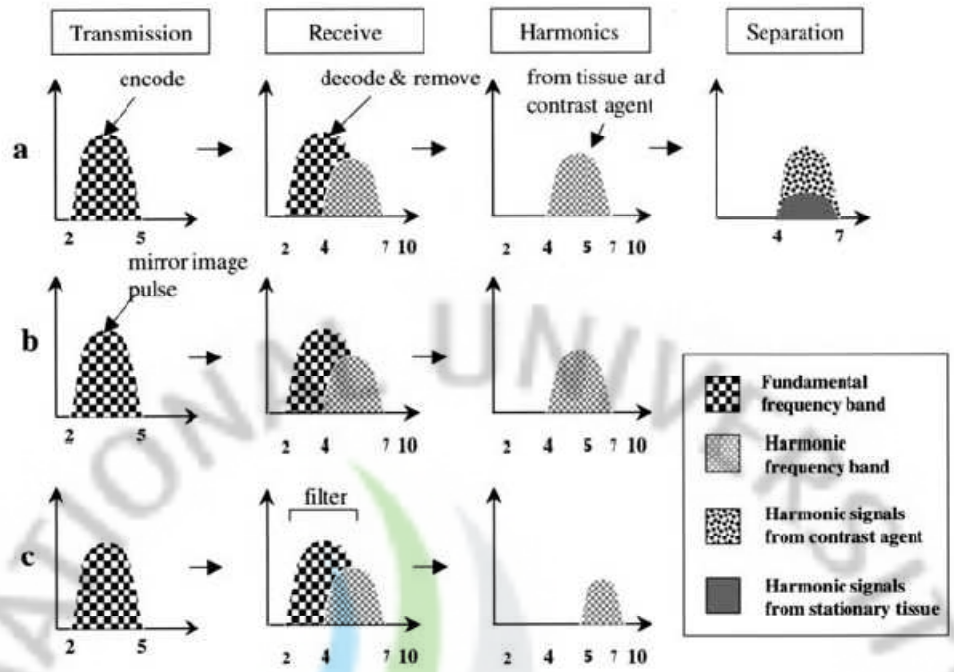

Fig. 2.1 Principle of harmonic imaging: comparison with pulse-inversion and conventional harmonic technique. (a) Coded harmonic imaging. (b) Pulse inversion harmonic imaging. (c) Conventional tissue harmonic imaging. [62]

However, cyclic variation in echogenicity from human carotid artery was only observed by coded harmonic imaging. It was suggested that coded harmonic imaging reduced the dynamic range between tissue and blood.

Firstly, harmonic signals from any large and slow-moving tissue cluster component can be distinguished from these received harmonic signals, and suppressed by a specialized decoding technique. So that both the harmonic signals from tissue and blood are within the main gray scale region [62].

Secondly, a decorrelation between the multiple firings causes fundamental echoes to leak and become visible, while the coded harmonic imaging is used to image moving tissue or

blood,. Coded harmonic images are obtained from the combination of the second harmonic signals from the tissue and the leaked fundamental signals from the blood. The second harmonic signals from the tissue are much smaller than the fundamental ones, such that they are similar to the leaked fundamental signals from the blood. It explains that coded harmonic imaging reduces the dynamic range between tissue and blood [1].

Chapter 3

ORIGIN OF THE CYCLIC VARIATION IN ECHOGENICITY FROM BLOOD

3.1 Introduction

Several research groups have suggested that the spatial organization of aggregating red blood cells is considered as the main determinant of the echogenicity of blood [58]. Under pulsatile flow, the variation of RBC aggregation over the lumen is responsible for cyclic and radial variation in echogenicity. However, only a few studies on *in vivo* measurements are available. The cyclic variation in echogenicity was observed from transverse images of the carotid artery through a commercialized ultrasound system GE LOGIQ 700 (Expert GE medical systems, Milwaukee, WI, USA) with an M12L linear probe [1, 11]. The smoke-like echogenicity from blood can easily be connected with the artifact, which often appears in B-mode imaging. Harmonic echogenicity variation was measured as a function of flow speed under steady flow in a mock flow loop to verify the origin of the variation in echogenicity. The observed cyclic variation in echogenicity from human carotid arteries was originated from the dynamic change of RBC aggregation due to the combined effects of flow acceleration and shear rate. In this research, the cyclic variation in echogenicity was observed from common carotid arteries using another ultrasound system and transducer. This study aims to validate the

observed cyclic variation of harmonic echogenicity reflecting ultrasound backscatter from blood and RBC aggregation. The echogenicity of porcine whole blood and RBC suspension was measured as a function of flow speed under steady flow.

3.2 Materials and Methods

Blood preparation

Fresh porcine blood was used in this experiment for its aggregation tendency is close to that of human blood compared with other species of livestock, e.g., horse, sheep, and cow [9]. Four fresh porcine blood samples were obtained from a slaughterhouse. Three gram of dipotassium salt (EDTA) dissolved in 30 ml of saline was used for anticoagulation of 1 liter of blood collected from each pig. Two different bloods were used in this experiment: non-aggregating porcine RBCs suspension in saline and aggregating porcine whole blood. Blood was centrifuged to separate the RBCs from the plasma. The buffy coat layer including white blood cells, platelets, and other minor cells was removed. The concentrated RBCs and autologous plasma were mixed and adjusted for the whole blood experiments to 40% hematocrit, where the aggregation is maximized [63-64]. To prepare saline RBC suspension, the porcine whole blood was centrifuged to separate the RBCs from the plasma. The plasma and buffy coat were removed and red cells were washed twice with 0.9% normal saline solution buffered to pH 7.4. Washed concentrated RBCs were then reconstituted with 0.85% saline solution to the desired hematocrit. In order to prevent crenation of the red cells, 0.5%

bovine albumin was added to the saline solution. The whole blood and RBC suspension were observed using a microscope, and the photomicrographs are shown in Fig. 3.1. RBCs formed rouleaux in porcine whole blood, but not in porcine RBC suspension.

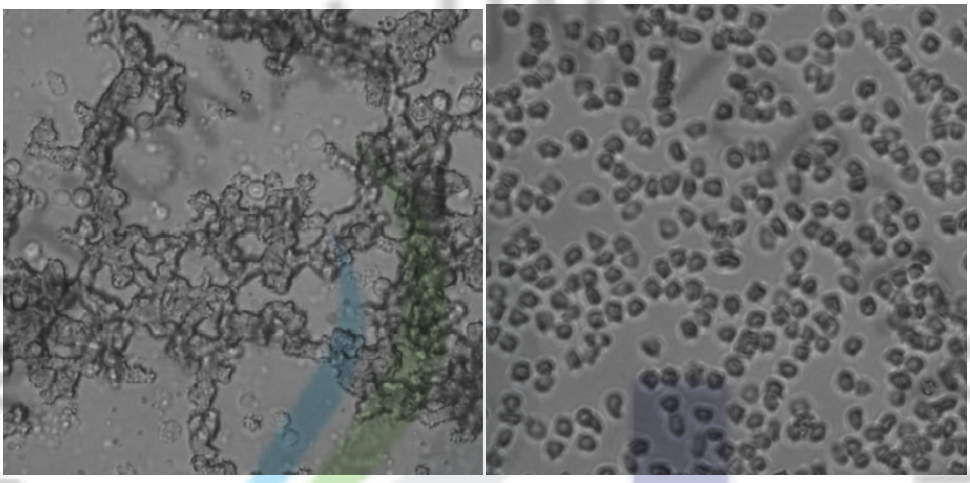

PWB PRBC

Fig. 3.1 Photomicrographs of porcine whole blood (PWB) and porcine RBCs suspension in saline (PRBC). Magnification × 500

Flow system

A mock flow system containing a commercial vascular phantom (Models 524, ATS Laboratories, Bridgeport, CT, USA) was made to generate steady flow. Two triangle beakers were used as reservoirs for the blood and to reduce speed fluctuations. The flow speed was controlled using a peristaltic pump (RP-1000, EYELA, Japan) and a silicon tubing (i.d. =7.94mm; o.d=11.11mm, EYELA, Japan) was used for connecting the vascular phantom with the two beakers and the peristaltic pump. The measuring site was chosen at one end of the

vascular phantom. The inlet length to the measuring site was 1 m, which was the requirement in generating laminar flow at the measuring site. The experiment setup of this experiment is presented in Fig. 3.2

Ultrasound system

A Voluson e ultrasound system with a broadband linear array scanner 12L-RS (frequency range: 4–12 MHz) was used to collect the image data. One transmit focus was applied for all the measurements. To obtain the best possible spatial resolution, the transducer was set to the highest frequency, image quality was set to high, and the highest available dynamic range was selected. No additional filtering was applied. Using these parameter settings, the maximum frame rate reached 32 frames/s. In a sequential image, 200 frames can be recorded maximally. Due to the limit in the total frame number in a sequence, a high frame rate sequence was preferred and the measurement time of each image sequence was kept to about 6 s. Voluson e ultrasound system and 12L-RS broadband linear array scanner are shown in Fig. 3.3 and Fig. 3.4, respectively.

(a) Vascular phantom

(b) Peristaltic pump

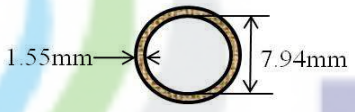

(c) Silicon tubing

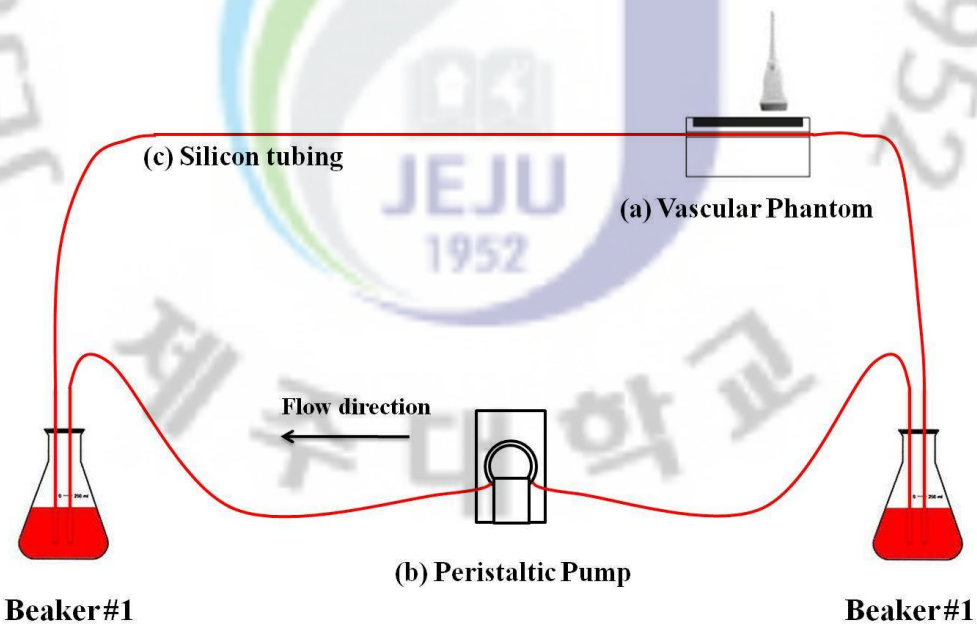

Fig. 3.2. Experimental arrangement for steady flow measurement

Fig. 3.3. Voluson e ultrasound system [65]

Fig. 3.4. 12L-RS Electronic broadband linear array transducer [66]

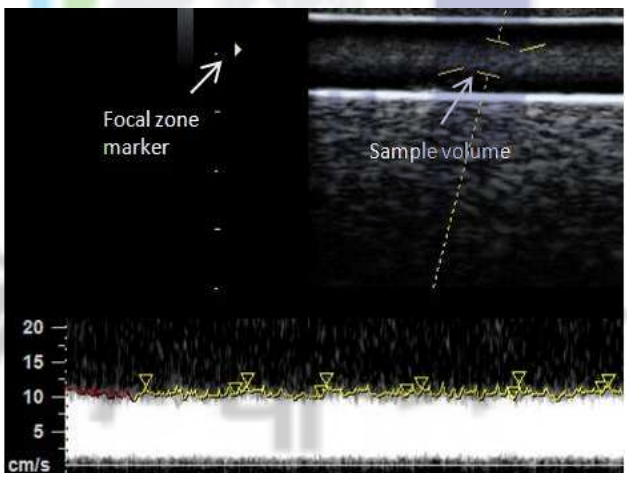

Fig. 3.5. A Duplex Doppler image collected by a GE Voluson e ultrasound system.

Data acquisition and analysis

Flow speed at the centerline of the tube was measured using the Doppler spectrogram in the duplex imaging. The sample volume was set to 3mm, and positioned over the central region of the tube channel. The focal zone was adjusted to the center of the channel, as shown in Fig.3.5. The rotation speed of peristaltic pump was varied by 18 levels for whole blood and 9 levels for RBC suspension, ranging from 0 to 300 rpm. The flow speed was measured by a duplex image and the corresponding echogenicity was recorded from 200 frames of harmonic images for both whole blood and RBC suspension at each rotation speed. The flow speeds of different blood samples were varied at the same rotation speed. To better visualize the results from whole blood, the echogenicity from whole blood as a function of flow speed was upsampled by a factor of 40 using the low-pass interpolation algorithm [67]. The interpolation functions were averaged to get the mean echogenicity from 4 different blood samples at each flow speed.

3.3 Results

The relation of harmonic echogenicity and blood flow speed in vitro

Echogenicity from the four porcine blood samples are displayed as a function of flow speed in Fig. 3.6. The solid line is the mean echogenicity from the four porcine whole bloods and the dashed line is the echogenicity from four RBC suspensions. The mean echogenicity from four whole porcine blood samples decreased from 79 to 7 as the flow speed increased

from 0 to 40 cm/sec. The echogenicity from erythrocyte suspension was found to range from 7.9 to 8.5 and did not vary much with flow speed up to 43 cm/sec, which is in agreement with previous results measured using a GE LOGIQ 700 Expert system with an M12L probe. Thus, the harmonic echogenicity from the blood acquired by a Voluson e ultrasound system reflects the ultrasound backscatter from blood and RBC aggregation.

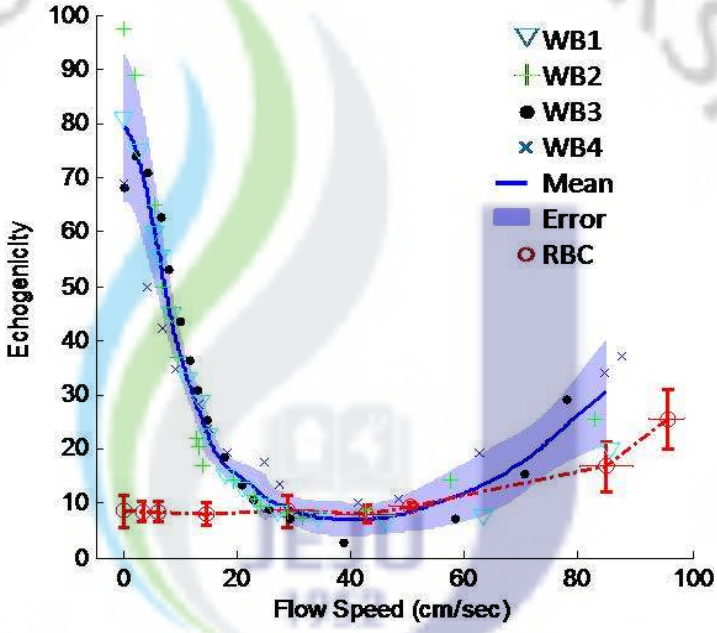

Fig. 3.6. The harmonic echogenicity from porcine whole blood (WB) and red blood cell suspensions (RBCS) as a function of flow speed. RBCS results are the mean ± standard deviation of four different blood samples. WB represents whole blood sample and the numbers represent the different bloods. Mean and Error represent the average interpolation function and the standard deviation from four whole blood samples, respectively. The interpolation function was obtained using a low-pass interpolation Algorithm [67].

However, echogenicity from whole blood increased from 7.1 to 30.6 when the flow speed increased from 40 to 85 cm/sec and the echogenicity from erythrocyte suspension also increased from 9.5 to 25.5 when flow speed increased from 51 to 96 cm/s. The increase in echogenicity in the whole blood and erythrocyte suspension at flow speed over 40 cm/sec may be attributed to the white speckles in the harmonic image at this high flow speed. The air bubbles appeared inside the two beakers, when flow speed is over 40 cm/s. The number of air bubbles gradually increased with the increase of the rotation speed of peristaltic pump. Therefore, those air bubbles were related with the turbulence caused by the blood flowing in and out of the beakers.

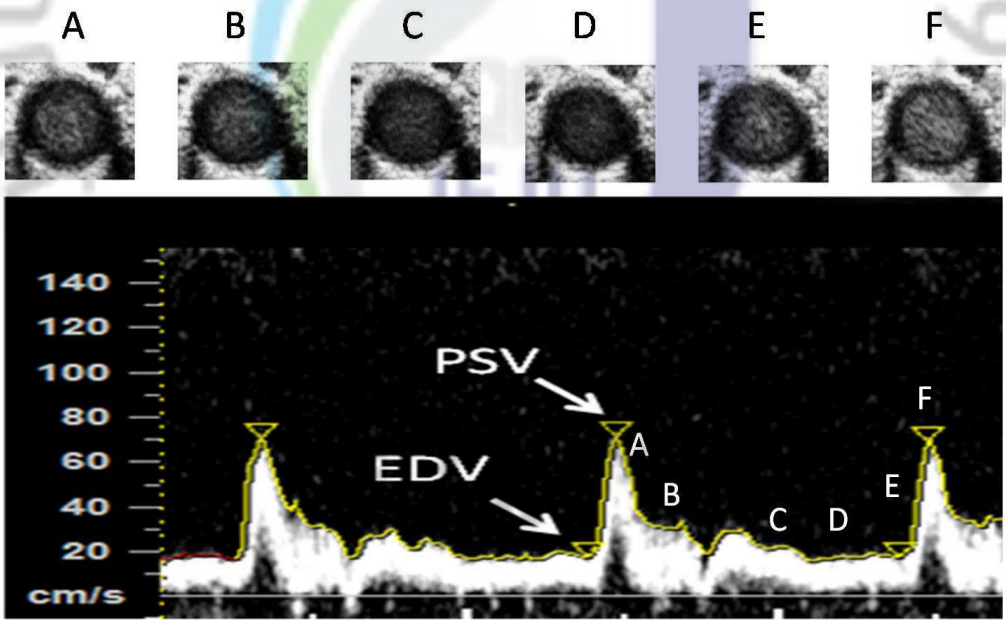

Fig. 3.7. Duplex Doppler image and the corresponding cross-sectional harmonic image of the common carotid artery in different phases. PSV: peak systolic velocity, EDV: end-diastolic velocity

Relationship between harmonic echogenicity and blood flow speed in vivo

Six harmonic images measured from the cross section of the common carotid artery of a healthy smoker with their corresponding blood flow speed are presented in Fig.3.9. The cyclic variations in echogenicity were maximal near the peak of systole. The pattern of the variations in harmonic echogenicity during the cardiac cycle is in agreement with previous results *in vitro* [51, 53, 68] and *in vivo* [1].

3.4 Discussion

Increased echogenicity at high flow speed

White speckles were generated at high flow speed, and lasted after the flow stopped. These speckles were observed in the harmonic image of the porcine whole blood when the flow speed of 80 cm/s was stopped (Fig. 3.8.a), but not when 40 cm/s was stopped (Fig. 3.8.b). The same phenomena were also observed in the RBC suspension.

White speckles gradually disappeared within 1-3 minutes after the blood flow was stopped. A sequence of harmonic images of RBC suspension was recorded after the blood flow over 100 cm/s was stopped. The harmonic images of RBC suspension right after, 20 seconds, and 2 minutes after flow stoppage are displayed in Fig. 3.9. The white speckles were found in the image right after flow stoppage (Fig. 3.9.a), reduced after 20 seconds (Fig. 3.9.b), and totally disappeared after 2 minutes (Fig. 3.9.c). The air bubbles in the beakers and the white speckles in blood image disappeared at the same time.

Therefore, the white speckles, which appeared in blood images at high flow speed, were generated from air bubbles in the blood flow. The increased echogenicity from whole blood and erythrocyte suspension at flow speed over 40cm/sec is mainly attributed to these air bubbles.

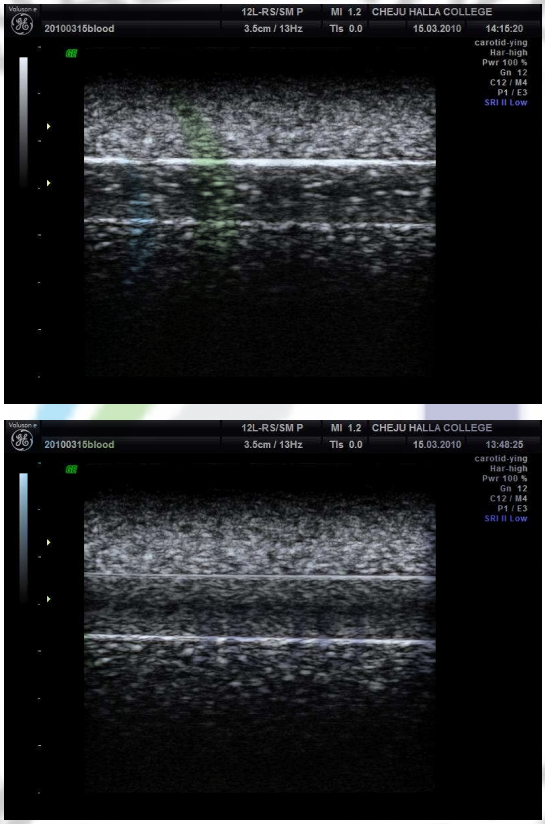

(b)

Fig. 3.8. Harmonic images of porcine whole blood in the vascular phantom (a) stopped from flow speed of 80 cm/s (b) stopped from the flow speed of 40 cm/s.

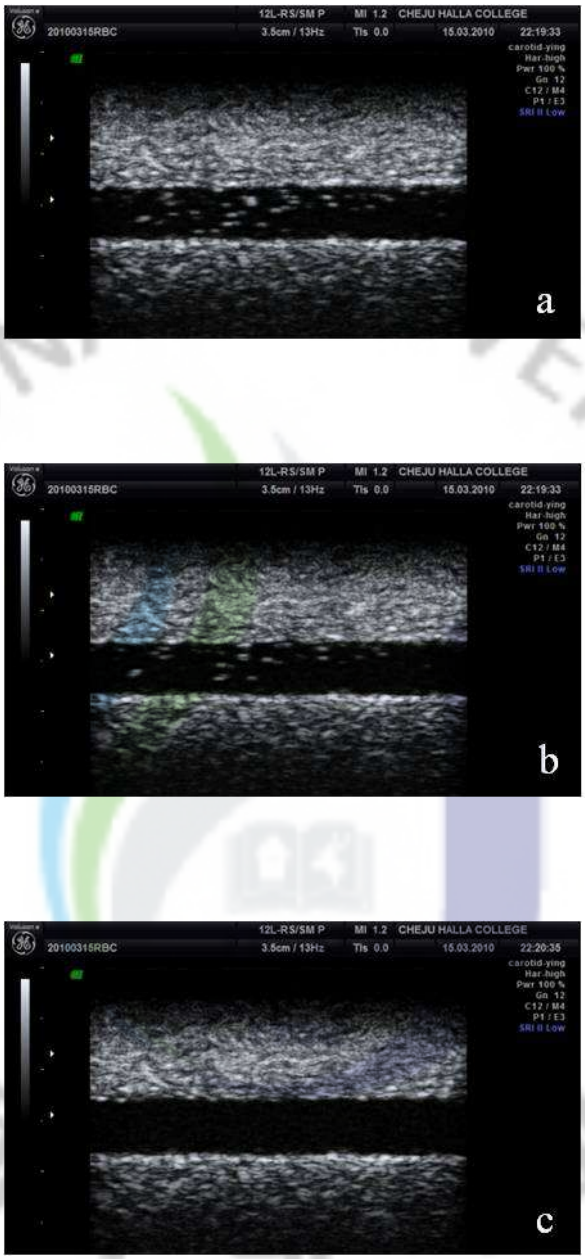

Fig. 3.9. Harmonic images of RBC suspension in the vascular phantom at static conditions, (a) blood flow stopped from high speed flow condition, (b) 20 seconds after the stoppage of blood flow, (c) 2 minutes after the stoppage of blood flow.

Origin of variation of echogenicity from blood

Harmonic images of aggregating porcine whole blood and non-aggregating RBC suspensions were measured as a function of flow speed under steady flow in a mock flow loop using the same ultrasound system with the same probe setup. The harmonic echogenicity of porcine whole blood was significantly higher than that of the RBC suspension at the same static flow rate. The harmonic echogenicity of porcine whole blood decreased exponentially as flow speed increased from 0 to 40cm/s, whereas the echogenicity of the non-aggregating RBC suspension was not correlated with flow speed. These results are in agreement with previous observations [1]. Shear rate is the most important hemodynamic factor affecting RBC aggregation. The integrated backscatter power and the echogenicity of blood are dependent on shear rate in a Couette flow system [69] and flow velocity in a mock flow system [57]. RBC rouleaux are broken up at high shear rates. Hence, shear rate-dependent RBC aggregation is considered the main reason for variations in echogenicity under steady flow.

Blood flow through the common carotid artery was different from the *in vitro* porcine whole blood under steady flow. Under pulsatile flow, blood echogenicity [53, 70] and backscatter power [56] decrease at high flow speeds. Increased shear rate at high flow speed prevents the formation of RBC rouleaux, reducing the backscatter or echogenicity. However, the maximum echogenicity of blood in a pulsatile cycle is found near the peak velocity in *in vitro* [51, 53, 56, 68] and *in vivo* [1] studies. A similar pattern was observed in this study (Fig.3.9). There are two possible explanations for this pattern: (1) The blood velocity profile of

the common carotid artery was reported to be flat during the systolic peak and parabolic during diastole and early systole (Velocity profile 2 in Fig.3.10.C and Fig.3.11.A) [71-72]. The flattened flow speed decreased shear rate near the center of the artery, consequently increasing RBC aggregation. This could explain the increased echogenicity near the center of the artery at peak systole, but it cannot explain the low echogenicity at the late diastole wherein flow speed and shear rate are small (Velocity profile 8 in Fig.3.10.C and Fig.3.11.D). (2) Flow acceleration was suggested as a possible factor that can increase the echogenicity of blood [50, 53-54, 70]. The combined effect of flow acceleration and shear rate was suggested as the possible explanation for this cyclic pattern [1]. The high flow acceleration and low shear rate may further explain the increased echogenicity at peak systolic. However, the mechanisms of how flow acceleration increases the blood echogenicity are still unclear and need further exploration. Cloutier and Shung [50] emphasized the effects of turbulence introduced by flow acceleration. However, very little *in vivo* evidence that there was turbulence, which would mostly occur during deceleration phase, was found. Paeng et al. [53] suggested that the increased echogenicity near peak systole should be mainly attributed to the enhanced RBC aggregation due to compression forces and greater collision rate of RBCs in flow acceleration. Additionally, RBC and RBC rouleaux were suggested to be aligned at a certain angle in steady flow [73] and during the acceleration period *in vitro* [73-74]. Hence the orientation of RBC and RBC rouleaux is another possible factor contributing to the increase of echogenicity at peak systole

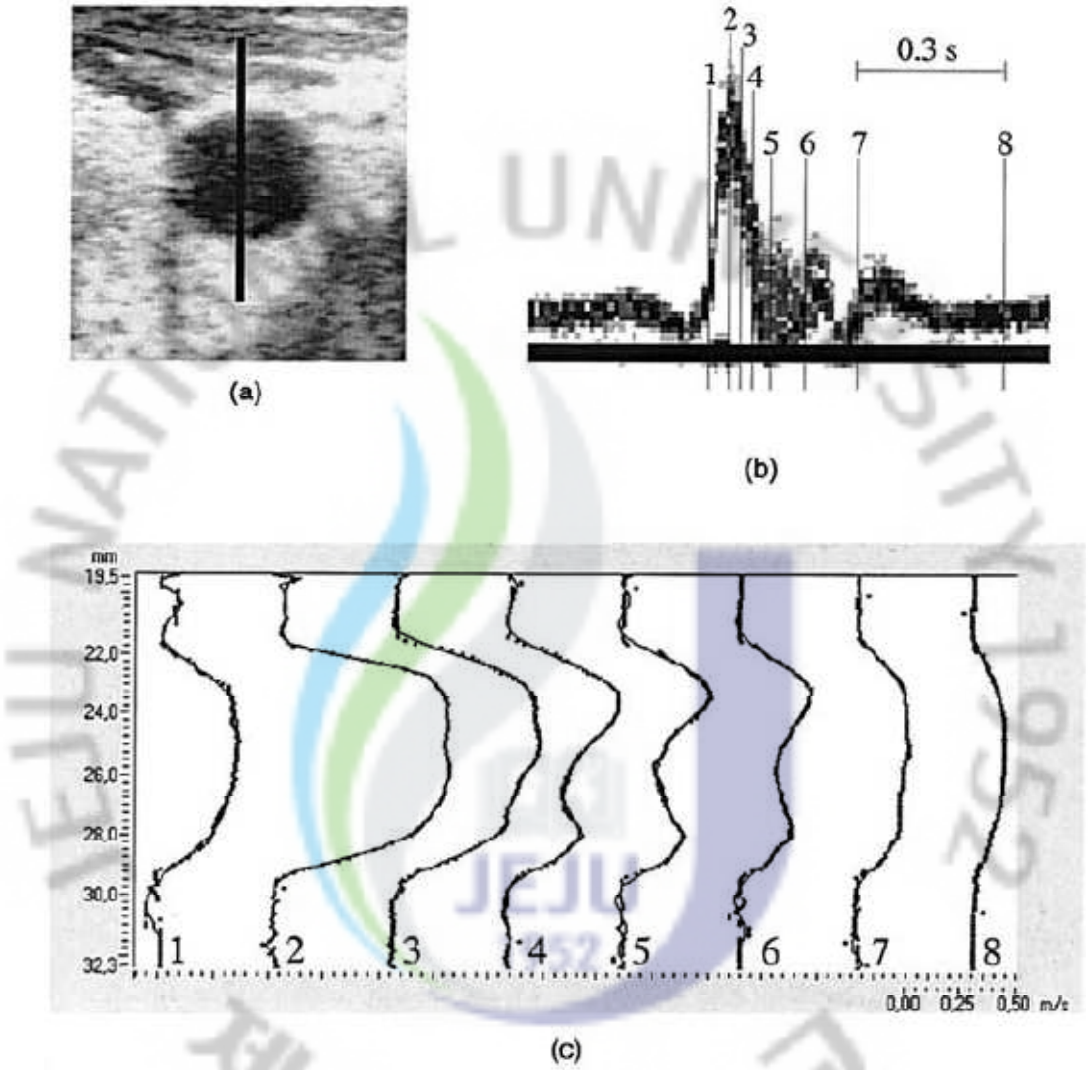

Fig. 3.10. (a) Investigated arterial cross-section: the scan line over which multigate analysis was performed is highlighted. (b) Reference spectrogram of the Doppler signal produced by the maximum streamline velocity intercepted along the multigate scanline. (c) Velocity profiles corresponding to time instants highlighted in (b). [71]

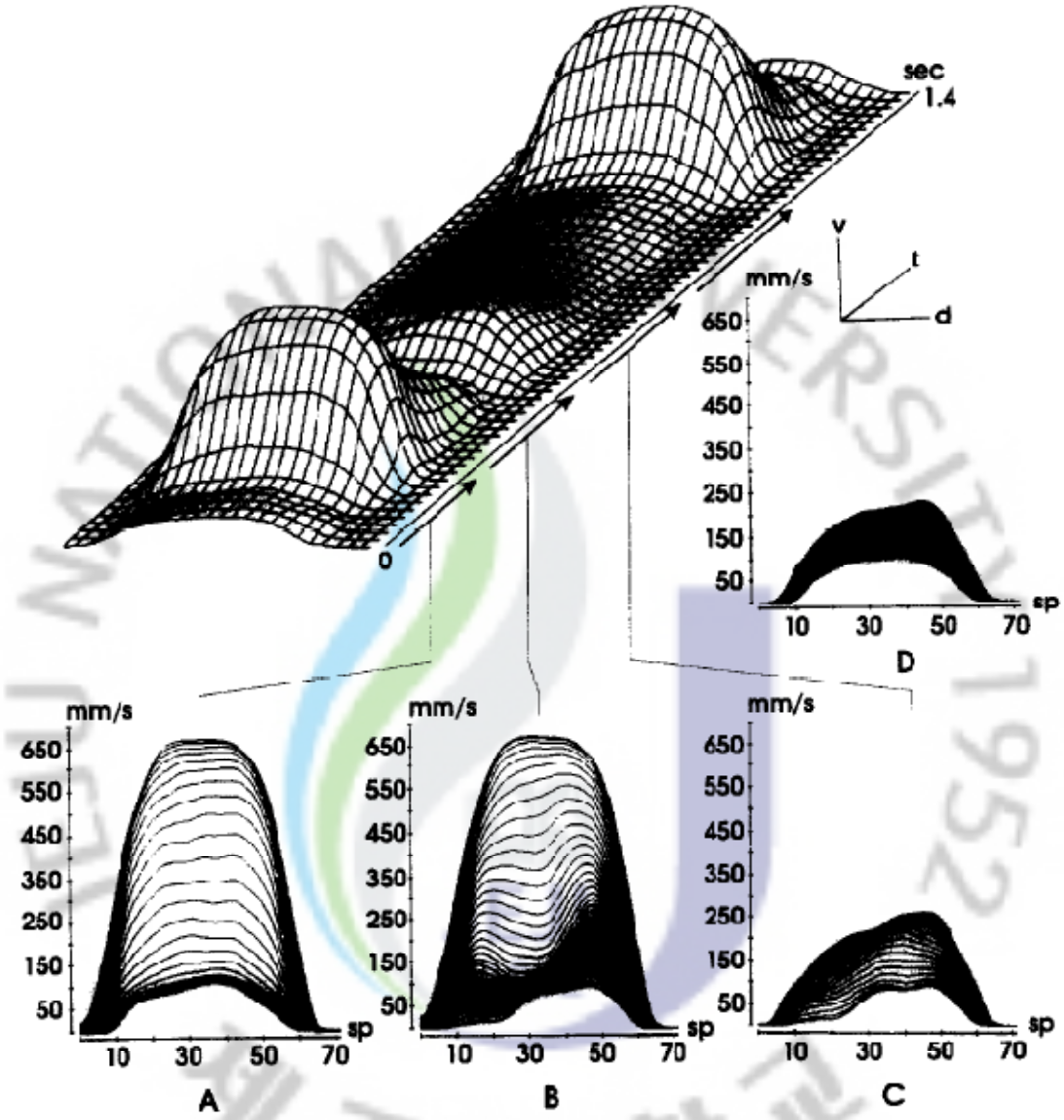

Fig. 3.11. The time dependent blood flow velocity distribution as estimated from the raw ultrasound information measured in the common carotid artery (D=6.5mm). Moreover, some blood flow velocity profiles as estimated at various moments in a heartbeat are shown: (A) Systole, (B) late systole, (C) mid-diastole, (D) late diastole. The unit used for the spatial axis is sample points (sp), and 1 sp is equal to 109 μm. [72]

3.5 Conclusion

The flow speed dependence of echogenicity from whole blood and RBC suspension up to flow speed of 40 cm/sec was in agreement with pervious measurement from harmonic echogenicity collected by a GE LOGIQ 700 Expert system with an M12L probe (Fig.1.4) [1], Doppler power collected by a 10-MHz pulsed Doppler system (Fig.1.5) [53], and conventional B-mode echogenicity (Fig.1.6) [57]. Therefore, the harmonic echogenicity from the blood acquired by the Voluson e ultrasound system reflects the ultrasound backscatter from blood and RBC aggregation.

The increased echogenicity from whole blood and RBC suspension at flow speed above 40cm/sec is mainly caused by the air bubbles. However, those air bubbles would not appear *in vivo*, and would not be responsible to the variation of echogenicity from the artery. Flow acceleration and the orientation of RBC and RBC rouleaux may be attributed to the pattern of echogenicity *in vivo*. But RBC aggregation can still be considered as a determinant of the observed CVE of flowing blood from the common carotid artery.

Chapter 4

THE AMPLITUDE INDEX OF CYCLIC VARIATION OF ECHOGENICITY: A_{CVE}

4.1 Introduction

In this research, the cyclic variation in blood echogenicity was observed from cross-sectional images of the common carotid artery using coded harmonic imaging of a commercial ultrasound system. To evaluate the amplitude of the cyclic variation in blood echogenicity, the difference between the peak and mean echogenicity in a cycle was defined as the amplitude index, A_{cve}. Accurate measurement of the cyclic variation in echogenicity from blood is important in estimating blood properties, which change dynamically during a pulsatile cycle *in vivo*. This will help in understanding blood rheology and hemodynamics, and in developing a useful tool for real-time monitoring of certain blood-related diseases. To better extract the blood echogenicity from the common carotid artery, Hough Transform (HT) was applied to identify the blood vessel lumen from the cross sectional image of the carotid artery.

Hough transform(HT) was introduced by Hough [75], and is the one of the most popular tools for image segmentation. HT was applied in the line detection by Duda and Hart [76], circle detection by Kimme et al. [77], and arbitrary shape extraction by Ballard [78]. Those researches focused on applying HT to study the vascular geometry, morphology, and elasticity.

However, Nash et al. [79] and Wu et al. [80] applied HT to segment the arterial wall from ultrasound image and estimate the systolic and diastolic diameters from images of cross section of the arterial wall. Golemati et al. [81] applied HF to segment the arterial wall from ultrasound image sequences of longitudinal as well as cross sections of the carotid artery. HT allows assessing the changes of arterial wall geometry during a cardiac cycle.

The representation of a circle for the HF computation is specified as:

$$(x-a)^2+(y-b)^2=r^2 \tag{4.1}$$

Where (*a*, *b*) are the coordinates of the center and *r* is the radius of the circle. HF results have a larger number of candidate circles. The parameter set (a, b, r) of the cell with the maximal value in the accumulator array was used to define the vessel lumen.

4.2 Method

To evaluate the amplitude of the cyclic variation in blood echogenicity, a Matlab (The MathWorks Inc., Natick, MA, USA) code was developed to analyze the recorded harmonic image sequence. HF was applied to track the arterial wall sequentially. The blood image was extracted from the whole image for each frame to calculate $A_{cve.}$ The two main parts of this code are summarized below.

Identify the arterial wall

The method of Golemati et al. [81] was modified to identify the arterial wall in the cross

section of the carotid artery image. The main steps of arterial wall identification were briefly summarized as:

1. *Reduction of image area:*

Reduction of image area is important for the error of circle detection is minimized and calculation cost is reduced. First, the small structures are filtered out by morphological opening, threshold gray image to binary image, remove a homogenous low-intensity area and define four points N1, N2, N3, N4, by the first and last nonzero columns and rows to delimit the area to be investigated. Original image was isolated by a rectangular area, which is delimited by previous defined four points. The vessel lumen part was remained, and the rest was removed.

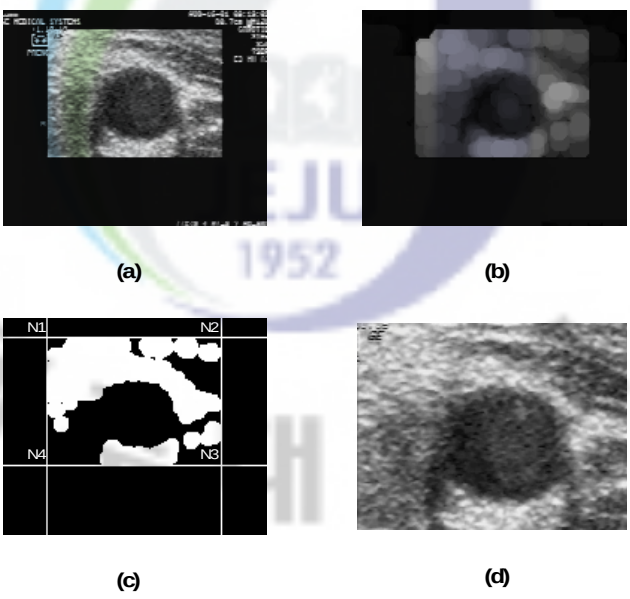

Fig 4.1. Procedure for the reduction of image area to segment. (a) original image, (b) image after morphological opening, (c) convert to binary image and define the cropping boundary, (d) image after reducing area.

Fig.4.1 shows an example of the procedure for reducing the image area. Fig.4.1.a is the original image. Fig.4.1.b is the image after morphological open. Fig.4.1.c is a rectangular area defined by four points in the binary image after thresholding. Unwanted structures were cropped by this rectangle. The resulting image is shown in Fig.4.1.d and will be used for the further steps to detect the boundary of blood vessel and extract useful information.

2. *Image process:*

A symmetric Gaussian low-pass filter with kernel size 7×7 pixels and $\delta_x=\delta_y=1$ was applied to remove high frequency noise. Morphological closing was performed to merge small "channels" and "opening" of the image. Morphological reconstruction algorithm was applied to clear the border of a binary image [82].

3. *Edge detection:*

A global threshold was selected automatically based on an interactive technique. It was developed by Ridler and Calvard [83] .The gray values in an image were initially segmented into two clusters using a starting threshold value as half the maximum dynamic range. The sample mean (mf_0) of the gray values associated with the pixels in the first cluster and the sample mean (ms_0) of the gray values associated with the pixels in the second cluster are computed. A new threshold value L_0 is now computed as the average of these two sample means.

$$L_0 = \frac{mf_0 + ms_0}{2} \quad (4.1)$$

$$L_1 = \frac{mf_1 + ms_1}{2} \quad (4.2)$$

…

$$L_n = \frac{mf_n + ms_{n1}}{2} = L_{n-1} \quad (4.3)$$

The process is repeated, based upon the new threshold, until the threshold value does not change any more. The Sobel gradient operator was applied to detect the boundary of the resulting binary image.

4. *Hough Transform:*

The HT was applied to the binary images produced after edge detection. Details were described in previous studies [79-81]. Fig.4.1.a shows the original image (after reduction of image area) as shown in Fig.4.2.d. Fig.4.2.b shows the image after Gaussian low-pass filtering. Fig.4.2.c shows the image after morphological closing. Fig.4.2.d shows the binary image after thresholding. Fig.4.2.e shows the image after morphological reconstruction. Fig.4.2.f shows the detected edge image in binary image. Fig.4.2.g shows the detected circle image in binary image. Fig.4.2.h shows the detected circle image on the original image.

The amplitude index of cyclic variation of echogenicity: A_{cve}

A detected circle using Hough transform is shown in Fig. 4.1. The detected circle was assumed as the boundary of the arterial wall. The average echogenicity (AE) was recorded from the central region-of-interests (Fig. 4.1.C), which is about 25% of the area of the whole

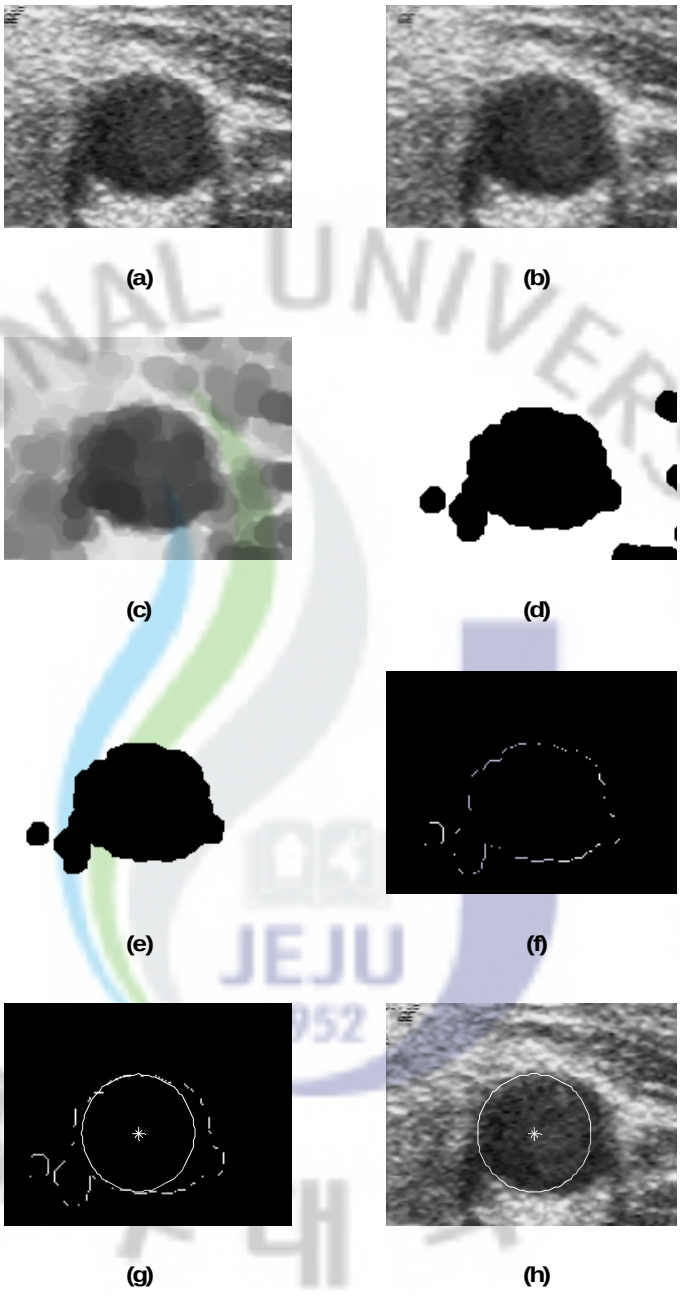

Fig 4.2. Procedure for applying HF to detect a circle. (a) original cropped image, (b) image after Gaussian low-pass filtering, (c) image after morphological closing, (d) binary image after thresholding, (e) image after morphological reconstruction, (f) binary edge image, (g) detected circle image in binary image, and (h) detected circle image on the original image.

vessel lumen in each frame. Fig. 4.2 shows the time sequence of AE. A_{cve} is defined as the difference between the peak and mean echogenicity in a cycle (Fig. 4.3). It is used as an index to describe the amplitude of the cyclic variation in echogenicity. All analysis codes were programmed using Matlab (The MathWorks Inc., Natick, MA, USA).

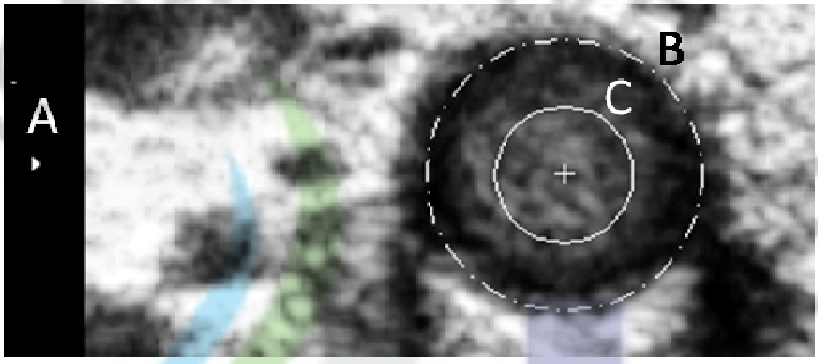

Fig. 4.1. A: Focal zone marker; B: Circle detected by HF; C: Circle to collect echogenicity

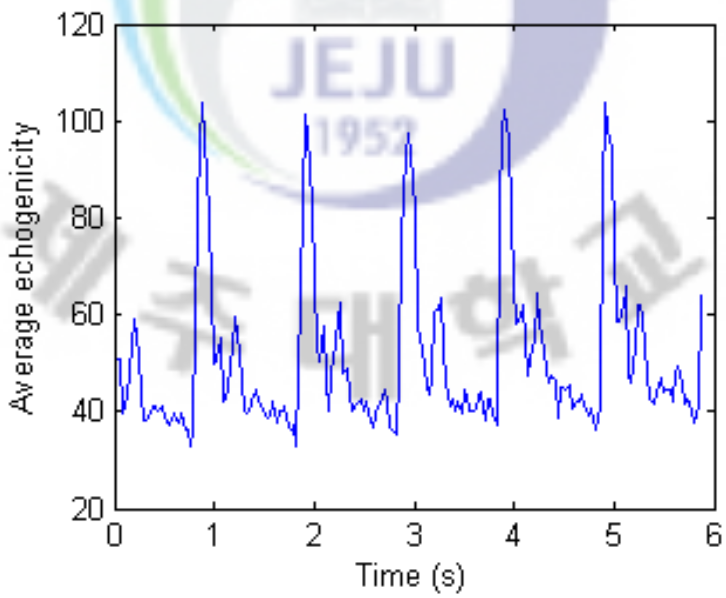

Fig. 4.2. Average echogenicity of blood in time domain.

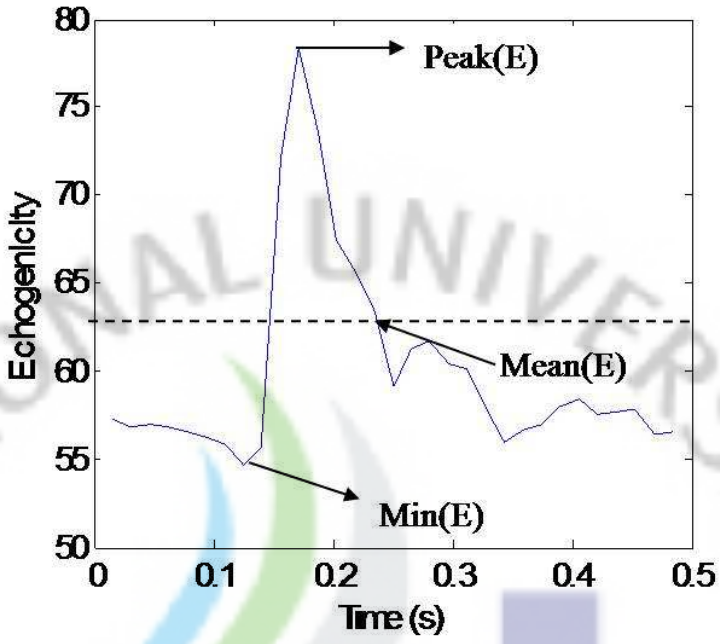

Fig. 4.3. A cycle of variation in echogenicity from ROI. Mean (E) presents mean echogenicity; Peak (E) presents peak echogenicity.

4.3 Discussion

Variations in RBC aggregation are responsible for CVE, and then A_{cve} is related to the dynamic changes in RBC aggregation during a cardiac cycle. Increased RBC aggregation is an independent risk factor for many diseases. Most studies on the rheological properties of RBC aggregation are based on the measurement of blood flow outside the vascular system. However, the *in vivo* properties of blood are significantly different from those *in vitro.* If it is assumed that the RBCs are totally disaggregated at a certain period of a cardiac cycle, then A_{cve} would be associated with the maximum RBC aggregation level. This provides a

theoretical basis for using A_{cve} in estimating RBC aggregation. Instead of evaluating the RBC aggregation under a defined shearing condition, A_{cve} can be used to estimate RBC aggregation *in vivo*.

However, A_{cve} is influenced by many other factors, e.g. the angle between the probe and neck, and the penetration thickness in tissues as the attenuated backscattered power is obtained from the blood by propagation through the intermediate soft tissue. It is important to note that the hemodynamic parameters, e.g., HR and BP also had significant effects on $A_{cve.}$ Therefore, to compare A_{cve} with the different subjects, these factors need to be considered.

4.4 Conclusion

A Matlab code based on HF was developed to automatically identify the arterial wall in the cross sectional image of the carotid artery. CVE was recorded from the central region of the artery, which was related with RBC aggregation *in vivo*. The amplitude of CVE was used as an index, namely A_{cve}. The potentials and limitations of A_{cve} to indicate the RBC aggregation tendency *in vivo* were suggested theoretically, and need to be tested in practice.

Chapter 5

THE ACUTE EFFECTS OF SMOKING ON A_{CVE}

5.1 Introduction

An abnormally high level of RBC aggregation is associated with many cardiovascular diseases and other pathologies [84-86]. RBC hyperaggregation has a direct effect on the formation of thrombi at low shear rates [2] and may create problems in microcirculation [3]. However, there are only few ways of measuring and monitoring this phenomenon noninvasively *in situ*. The potential of ultrasound as a useful noninvasive tool to study RBC aggregation has been predicted for a long time. Several research groups have shown *in vitro* that ultrasound backscattering from blood depends on RBC aggregation [7-10]. Another group has demonstrated *in vivo* that the backscatter is significantly higher in veins than in the arteries and significantly higher in patients with hyperlipidemia than in normal individuals [47]. However, the noninvasive *in vivo* dynamic changes in RBC aggregation under pulsatile flow are still unexplored.

In this study, the CVE was measured in 40 smokers using GE Voluson e ultrasound system (GE Medical Systems, Zipf, Austria) with a 12L-RS probe. Smoking was introduced as a stimulator of RBC aggregation *in vivo*. After smoking 1 cigarette, the heart rate (HR) of the subjects increased 5–10 BPM, and HR was restored after 90 min when no more nicotine was consumed [34-35]. Additionally, the systolic and diastolic blood pressure increased during

smoking [27-28]. Therefore, smoking could acutely influence blood flow, which would subsequently affect RBC aggregation. CVE and HR were measured and compared before and after smoking to explore the relationship among smoking, CVE, and RBC aggregation.

5.2 Methods

Experimental protocol

This study was approved by the Internal Review Board of the Jeju National University Hospital. Consent forms were signed by all participants after being briefed on the experimental process, the purpose of the study, and the possible risks involved. Each participant supplied their age, height, weight, state of health, cardiovascular disease history, exercise status, and smoking status. The volunteers were asked neither to take any food nor to smoke on the day of the examination until after the measurements were taken. The volunteers were also asked not to drink alcohol the night before the experiment. All the participants were male college students or teachers with no reported health problems and histories of cardiovascular diseases. All the measurements were taken in the morning by the same investigator. Each participant was examined 5–10 min before smoking and 10–60 min after smoking. During the examination, the individual participants were asked to rest for at least 5 min while lying comfortably on a bed. A linear array scanner was held by the investigator and placed on the neck near the common carotid artery after the application of a commercial coupling gel. Participants were then asked to stay still during the examination. The focus zone

of the probe was set to the appropriate position of the artery in the image. Gentle pressure was applied to the probe while aligning the focus zone marker to the center of the artery. The angle between the probe and neck was carefully adjusted to keep a round shape in cross-sectional images of the vessel and to remove the artifact inside the blood vessel. The parameter settings of ultrasound system were same with that of *in vitro* experiment in Chapter 3. A harmonic image of the common carotid artery is shown in Fig. 4.1. After the periodic variations in echogenicity stabilized, 5 harmonic image sequences were recorded. Additionally, 5 Doppler spectrum images were recorded for 14 smokers. The image data were transferred to a personal computer for post-processing using Matlab.

Data Analysis

To evaluate the HR and the amplitude of the blood CVE, a Matlab code was developed to analyze the recorded harmonic image sequences. The details on this code are summarized in Chapter 3. The time difference between two consecutive peaks of echogenicity was used to estimate HR. About 5–9 cardiac cycles were recorded in an image sequence and at least 5 recordings were taken for one measurement. A final result of A_{cve} and HR was averaged from approximately 30–50 values.

Statistical Analysis

In this study, A_{cve} and HR were compared before and after smoking. The changes in A_{cve} and HR after smoking were defined as ΔA_{cve} and ΔHR, respectively.

To reveal the population natural clusters among the smokers, the smokers were optimally divided into two groups through the two-step cluster analysis (TSCA). ΔA_{cve}, smoking years (SY), and average daily consumption of cigarettes (DCC) were used to differentiate the subjects. TSCA was performed using the demo version of Statistical Product and Service Solutions for Windows (IBM SPSS, Chicago, IL, USA). TSCA is an exploratory tool that reveals the natural clusters within a data set that would not be apparent otherwise. It is a scalable cluster analysis algorithm that uses a hierarchical clustering method. It can handle both continuous and categorical variables and has two steps: 1) pre-cluster the smokers into many small sub-clusters and 2) cluster the sub-clusters from step 1 into the desired number of clusters. Details on the TSCA have been described in Chiu et al. [87].

5.3 Results

Originally, 40 smokers participated in this experiment. However, 6 drank alcohol the previous night, 4 smoked in the morning, and 2 both smoked and drank alcohol. These 12 were excluded, leaving only 28 smokers for the analysis. Their ages ranged from 19–40 (mean=27.5±1.0), DCC from 1–30 (mean=12.56±1.7), SY from 1–20 (mean=7.8±5.8), and weekly exercise hours (WEH) were from 1–14 (mean=4.7±4.4).

Mean of A_{cve} and HR before and after smoking

The mean A_{cve} and HR of the 28 smokers increased from 25.8±10.7 to 28.7±10.5 and from 62.24±8.3 BPM to 65.4±7.9 BPM, respectively, after smoking. Among them, A_{cve}

increased in 22 smokers and decreased in 6 smokers. The HRs of 21 smokers increased and decreased in 7 smokers. Both A_{cve} and HR decreased in two smokers. Overall, A_{cve} and HR showed a tendency to increase. Results of A_{cve} and HR before and after smoking are summarized in Table 5.1.

Hemodynamic parameters before and after smoking

It was reported that increased HR increases both systolic and diastolic blood pressure and such direct association is stronger for systolic than for diastolic values of blood pressure [46]. The blood pressure might have influenced blood flow speed. Therefore, blood flow velocities of 14 smokers were recorded from the center of artery before and after smoking. All peak systolic velocities (PSV) and most of end-diastolic velocities (EDV) increased after smoking, validating the increased systolic and diastolic blood pressure [27-28]. The changes in PSVs and EDVs after smoking are correlated with the changes in HRs (Fig. 5.1 and Fig. 5.2). This suggests that the increase in HR may increase the mean blood flow velocity in the center of artery. Consequently, the mean shear rate of blood flow may be increased, which could prevent the formation of erythrocyte rouleaux and reduce the variations in RBC aggregation. In contrast, PSV increased more than EDV and the duration of the cardiac cycle decreased as HR increased. As a result, the blood flow velocity increased more in a shorter time and thus the acceleration in blood flow increased.

Table 5.1. Summary of A_{cve} and HR before and after smoking

Variable	Before smoking	After smoking
A_{cve}	25.8±10.7	28.7±10.5
HR (BMP)	62.2±8.3	65.4±7.9

A_{cve} =the amplitude of cyclic variation in echogenicity HR=heart rate

Table 5.2. Mean and Stand deviation of ΔA_{cve}, cigarettes/day, and smoking years of Clusters 1 and 2

Variable	**Category**	
	Cluster 1 Heavy smoker group (n=17)	Cluster 2 Mild smoker group (n=11)
ΔA_{cve}	4.98±4.26	-0.31±3.91*
DCC	18.1±6.0	4.0±4.1**
SY	8.5±5.2	7.5±7.1
Age	26.8±4.9	28.6±5.2
WEH	4.4±4.7	5.2±4.0
ΔHR	3.3±5.8	2.9±4.1

ΔA_{cve}=change of A_{cve}, DCC=daily consumption of cigarettes, SY=smoking years, WEH=weekly exercise hours, and ΔHR=change of heart rate ($^{**}p<0.0001$; $^{*}p<0.005$).

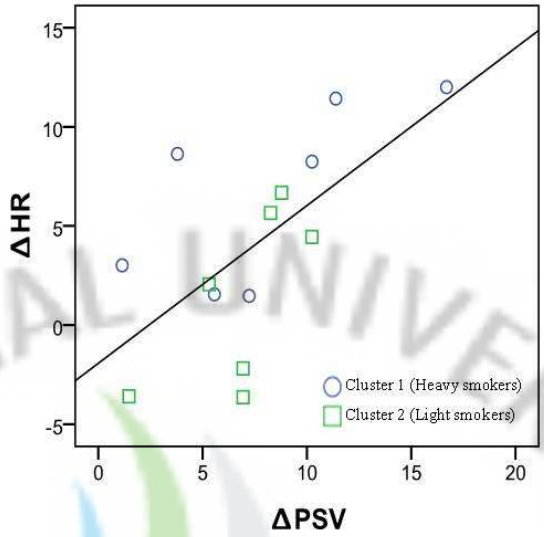

Fig. 5.1. Scatter plot of ΔPSV due to smoking and ΔHR with a least-square regression line

Y=-1.9 +0.8X (R=0.64, N=14, P<0.05)

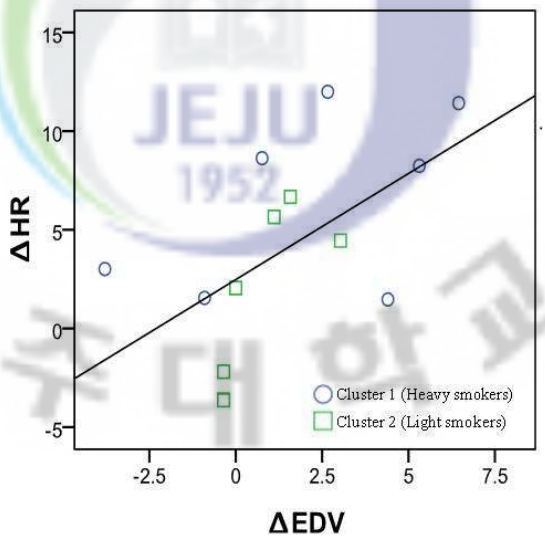

Fig. 5.2. Scatter plot of ΔEDV due to smoking and ΔHR with a least-square regression line

Y=2.5+1.3X (R=0.58, N=14, P<0.05)

TSCA

Based on ΔA_{cve}, DCC, and SY, the smokers were optimally divided into two clusters through the TSCA. The two clusters were compared using Student's t-test and results are summarized in Table 5.2. The differences between the two clusters were statistically significant for both ΔA_{cve} ($P<0.005$) and DCC ($P<0.0001$). However, no significant differences between the two groups in terms of SY, age, and WEH were found. The most significantly different parameter, DCC, between the two clusters was used to classify the two groups into heavy smokers and light smokers.

Cluster 1 or the heavy smoker group (n=17) generally consumed more cigarettes per day (DCC =18.12±6.03). Its average number of smoking year was 8.5±5.2.

Cluster 2 or the light smokers group (n=11) generally consumed less cigarettes per day (DCC =4.00± 8.78). Its average number of smoking year was 7.5±7.0.

TSCA revealed that the heavy smokers had significantly larger increases in A_{cve} (ΔA_{cve}=4.98±4.26) than light smokers (ΔA_{cve}=-0.3±3.01). This indicates that the heavy and light smokers may have different reaction in A_{cve} values after smoking. Scatter plots of ΔA_{cve} vs. ΔHR and ΔA_{cve} vs. DCC of cluster 1 and cluster 2 were displayed in Fig. 5.3 and Fig. 5.4, respectively.

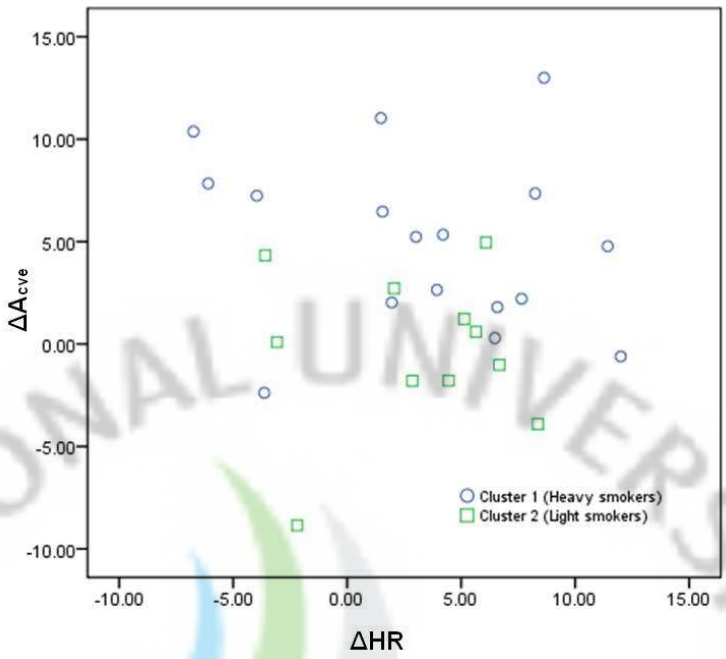

Fig. 5.3. Scatter plot of ΔA_{cve} vs. ΔHR of cluster 1and cluster 2 due to smoking

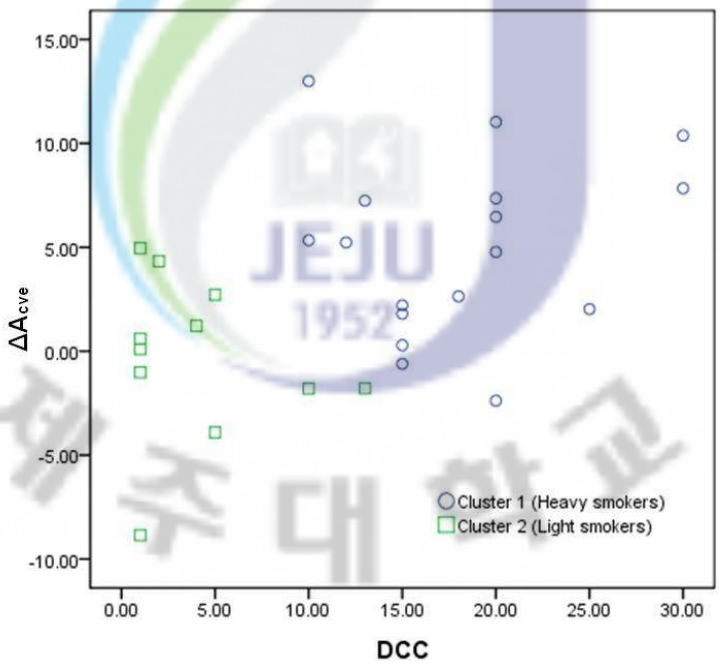

Fig. 5.4. Scatter plot of ΔA_{cve} vs. daily consuming cigarettes (DCC) of cluster 1and cluster 2

5.4 Discussion

Principal findings

This is the first measurement and analysis of the *in vivo* change of CVE in blood due to smoking using the harmonic images collected by a GE Voluson e ultrasound system. Generally, A_{cve} and HR increased overall after smoking. The heavy smoking group posted major increases in A_{cve}, whereas both groups posted similar increases in HR.

Acute HR change after smoking

HR increased in most of smokers. The increase in HR for the heavy smoker group ($\Delta HR=3.3\pm5.8$) was slightly higher than the mild smoker group ($\Delta HR=2.9\pm4.1$), even though the difference was not statistically significant. Some reports suggested that smoking impairs the baroreflex modulation of HR [28, 88]. Therefore, acute increases of HR as a response to smoking may be more observed for the relatively heavy smoker. To a certain extent, this tendency could be observed in Fig.5.4. In contrast, the increase in HR is significantly lower among smokers consuming more than 30 cigarettes per day than among light smokers [89]. The heavy smokers, i.e., those who consumed over 30 cigarettes per day, could have developed a substantial cardiovascular tolerance to the nicotine. However, only two volunteers reported more than 30 cigarettes per day in our study, and the differences in HR between the heavy and light smoker groups were not statistically significant in our study. Additionally, the increase in HR after smoking is dependent on the dose [36-37] and

subject-specific factors such as age [38], gender [39-41], blood type [42], hostility [43], and circadian typology [44]. Most of the smokers who participated in this study were male college students. Consequently, no significant difference in age between the heavy and light smoker groups was established. Therefore, the effects of gender and age on HR could not be attributed. However, other personality differences were not considered in this study.

Acute ΔA_{cve} changes after smoking

Overall, A_{cve} increased from 25.8±10.7 to 28.7±10.5 after smoking. The heavy smoker group had significantly larger increase in A_{cve} (ΔA_{cve}=4.98±4.26) than the light smoker group (ΔA_{cve}=-0.3±3.01). *In vitro* experiments revealed that the cyclic variations in echogenicity and backscattering power from pulsatile blood flow are more evident at low stroke rate and low peak flow speed [55-56]. The increased stroke rate and peak flow speed could lead to an increased mean shear rate, (Huang 2009) consequently, reducing the RBC aggregation. Therefore, the overall increase in HR should cause an overall decrease in A_{cve}, which was not exhibited by the results. The increased flow acceleration, which may enhance RBC aggregation, could possibly contribute to the increase in A_{cve}. However, significant difference in A_{cve} between heavy smoker group and light smoker group is still not attributed. Besides hemodynamic parameters, other factors may have caused the increase in A_{cve} after smoking.

Smoking could acutely affect some hematologic parameters to increase A_{cve}. Firstly, smokers have significantly increased RBC aggregation compared with non-smokers [17-18,

23]. Significant differences between smokers and non-smokers in terms of hematologic parameters, such as whole blood viscosity [20], fibrinogen concentrations [19-22], and hematocrit [19-20] have been established. These hematological parameters are known to have significant effects on the ultrasound backscattering from blood [7]. Secondly, the forearm vascular resistance [27] and calf vascular resistance [28] increased during smoking. Therefore, this increased vascular resistance possibly reflects the increase of RBC aggregation and blood viscosity. Thirdly, the blood flow resistance in common carotid artery increased during the graded exercise [90]. The RBC aggregation and blood viscosity acutely increased after exhausting exercise [91-92]. The increased RBC aggregation and blood viscosity may be major reasons affecting flow resistance in vessels by the exercise as they are affected by smoking, even though exercise and smoking effects are not the same.

Potentials and limitations of A_{cve}

A_{cve} has been demonstrated to be sensitive to possible alterations in RBC aggregation induced by smoking. The CVE observed through harmonic imaging is a potential tool in studying acute physiologic changes caused by smoking. In addition, the alterations in RBC aggregation were proposed as the mechanism of CVE. Therefore, A_{cve} is related to the dynamic changes in RBC aggregation during the cardiac cycle. As discussed in Chapter 3, by assuming that the RBCs are totally disaggregated at a certain period during a cardiac cycle, A_{cve} can be used to indicate the maximum RBC aggregation level. Instead of evaluating the

RBC aggregation under a defined shearing condition, A_{cve} can be used to define RBC aggregation. Increased RBC aggregation is an independent risk factor for many diseases. However, the mechanisms involved in the development of these diseases are still unclear. Most studies on the rheological properties of RBC aggregation are based on the measurement of blood flow outside the vascular system. However, the *in vivo* properties of blood are significantly different from those *in vitro*. The current study may help in the development of a potential index to study the dynamic changes in red blood cell aggregation *in vivo* using noninvasive ultrasound technology. However, this result was taken from a limited sample size, so further statistical research is required.

Some difficulties involved in using A_{cve} as a diagnostic tool is present. First, comparing the A_{cve} measured through different ultrasound systems is difficult because each system uses a different technique for harmonic imaging and interprets the backscattering power to echogenicity. Second, A_{cve} is affected by the penetration thickness in tissues as the attenuated backscattered power is obtained from the blood by propagation through the intermediate soft tissue. To compare A_{cve} with the different subjects, compensating for the loss of energy by attenuation is necessary. A_{cve} obtained in this study was not compensated by the attenuation, however, ΔA_{cve}, can be compared among different smokers because it is the relative change in A_{cve} caused by smoking. Future studies should focus on the development of effective methods in compensating for the difference in attenuation and to normalize the backscattered power of blood to be able to compare measurements among different subjects.

5.5 Conclusions

Smoking could acutely change blood echogenicity during a cardiac cycle and changes in CVE were different for the heavy and light smokers. The acute effect of smoking on the hemodynamic change could not be fully explained by the changes in CVE. The acute response of RBC aggregation and blood viscosity to smoking was suggested as an interpretation. Moreover, the acute response of RBC aggregation and blood viscosity to smoking would be different for the heavy smoker and the light smoker. However, more solid evidences for A_{cve} as an indicator of RBC aggregation *in vivo* and the further investigation on the changes in the hematologic parameters in acute response to smoking are needed.

Chapter 6

THE DIFFERENCE OF ACVE BETWEEN SMOKERS AND NONSMOKERS

6.1 Introduction

In the previous chapter, A_{cve}, the amplitude of variation in echogenicity, was measured in 28 smokers, before and after smoking. Both A_{cve} and HR increased after smoking. Smoking may acutely increase RBC aggregation tendency and the increase in A_{cve} may possibly be originated from the increase of RBC aggregation tendency

RBC aggregation levels at both low and high shear rate were significantly higher in smokers compared with nonsmokers [17-18, 23]. Several hematological parameters related with RBC aggregation were also found to be elevated in smokers compared with nonsmokers, such as plasma viscosity [15-17], whole viscosity [16-17], hematocrit [17-19], and fibrinogen concentrations [16-17, 19-22]. Furthermore, blood pressure (BP) and HR are also significantly higher in both male and female smokers and in male smokers alone compared with nonsmokers [24]. Increased BP and HR would influence blood flow, and subsequently affect RBC aggregation. Hence, chronic cigarette smoking could affect RBC aggregation by changing both hematological and hemodynamic conditions.

This study aims to test if smoking could chronically affect A_{cve}. The blood echogenicity

in common carotid artery was recorded from 20 male nonsmokers and 28 male smokers. Two parameters, i.e., A_{cve} and M_{cve} (Minimum echogenicity in a cycle), were calculated and compared between smoker and nonsmoker. The effects of tissue attenuation on A_{cve} and M_{cve} were compensated with body mass index (BMI) and then compared. Aggregation indices were also measured and compared between 8 male nonsmokers and 10 male smokers using a microchip-based laser aggregometer.

6.2 Methods

Volunteer population

20 nonsmokers and 28 smokers were invited to participate in this study. The nonsmoker is defined as someone who never became a habitual smoker and consumed less than 5 cigarettes in the past three years. Most of smokers were daily smokers with daily consumption of cigarettes (DCC) of 1–30 (mean=12.56±1.7) and smoking years (SY) of 1–20 (mean=7.8±5.8). These smokers were optimally divided into heavy smokers group (n=17, DCC=18.1±6.0, SY=8.5±5.2) and light smokers group (n=11, DCC=4.0±4.1, SY=7.5±7.1) through the two step cluster analysis. Details on this method have been described in the previous section. All participants were male college students or teachers with no reported health problems and histories of cardiovascular diseases.

Ultrasound examination

All ultrasound examinations of smokers and nonsmokers were taken in the morning by

the same investigator. They were asked to fast overnight, and forbidden to drink alcohol the night before the experiment. The equipment setup, experimental approach, and analysis method are same with those described in the previous section. Five sequences of harmonic images from carotid artery were recorded from each person for periodic variations in echogenicity. Each sequence was recorded for about 6 s. Peak systolic velocities (PSV) and end diastolic velocities (EDV) were recorded for 14 nonsmokers and 18 smokers.

Laser aggregometer examination

A microchip-based aggregometer, Rheo Scan A (Rheo Scan, Seoul, Korea), was used to measure aggregation indices, AI (indicating the normalized degree of the accumulated aggregation) and T_{half} (indicating the aggregation velocity) [93]. Venous blood samples were obtained from 8 healthy male nonsmokers and 10 healthy male smokers.

Data Analysis

The average echogenicity (AG) was recorded from the central region-of-interests (Fig. 4.1. C), about 25% of area of the whole vessel lumen in each frame. The time sequence of AG is presented in Fig. 2. The time difference between two consecutive peaks of echogenicity was used to estimate HR. The HR and AG were calculated using a Matlab code as described in detail in chapter 4. A_{cve} is defined as the difference between the peak and mean of echogenicity in a cycle and M_{cve} is defined as the minimum echogenicity in a cycle (Fig. 4.2). A final result was averaged from approximately 30–50 cycles.

Compensation of the tissue attenuation

Ultrasound power is attenuated, while it propagates through the intermediate soft tissue. A_{cve} decreased with the increase in BMI (Fig.6.1)). The linear regression analysis indicated the correlation between A_{cve} and BMI is significant ($R=0.6$, $P<0.0001$). In this study, BMI was assumed to be associated with the attenuation from intermediate soft tissue. The linear regression equation was used to compensate for the effect of tissue attenuation on A_{cve}. The same method was applied to compensate for the tissue attenuation effects on M_{cve}. The compensated A_{cve} and M_{cve} are marked as A'_{cve} and M'_{cve}.

Table 6.1. Summary of personal information for participants

	Nonsmokers (n=17)	**Light smokers (n=11)**	**Heavy smokers (n=17)**
Age	25.6±3.3[a]	28.6±5.2	26.8±4.9
BMI	24.3±4.1	22.2±2.8	24.3±4.5
WEH	2.9 ± 2.0[a]	5.2±4.0	4.4±4.7
DCC	-	4.0±4.1	18.1±6.0
SY	-	8.53±5.2	7.45±7.1

BMI=body mass index; WEH=weekly exercise hours; DCC=daily consumption of cigarettes; SY=smoking years;

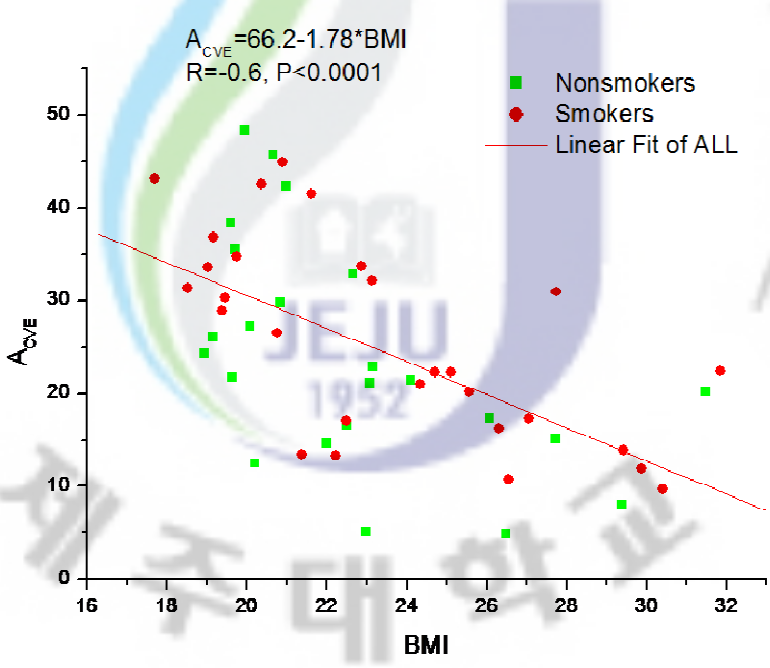

Fig. 6.1. Scatter plot of A_{cve} and BMI for all the participants, and least-square regression line

6.3 Results

Originally, 20 nonsmokers participated in this experiment. However, 3 proclaimed that they were exposed in environment of secondhand cigarette smoking very often due to their work and living environment and thus excluded. Finally, the data of 17 non-smokers, 11 light smokers, and 17 heavy smokers were used for comparison. Their personal information, including age, BMI, and weekly exercise hours (WEH) are summarized in Table 6.1. No significant differences among three groups in age, BMI, and WEH were found.

Comparison of A_{cve} and M_{cve} among three groups

Neither significant differences nor the change of tendency were found in A_{cve} and M_{cve} among 3 groups. However, the mean A'_{cve} was gradually increased from nonsmoker group (29.3±7.9) to light smoker group (35.2±5.1) and to heavy smoker group (36.7±9.5). Mean A'_{cve} was significantly higher in heavy smoker group and light smoker group compared with the nonsmoking group ($P<0.05$). In contrast, M'_{cve} was similar among 3 groups ($P>0.05$). The mean and standard deviation of A_{cve}, M_{cve}, A'_{cve}, and M'_{cve} of three groups are summarized in Table 6.2.

HR, PSV and EDV of smoking group and nonsmoking group

Nonsmoker group had smaller values in HR, PSV, and EDV compared with the other two groups. However, all three parameters were highest in the light smoker group. Moreover, HR and PSV are significantly higher in light smoker group (HR=64.0±7.7 (BPM);

PSV=105.1±16.9 (cm/s)) compared with the nonsmoking group (HR=58.0 ± 6.2 (BPM); PSV=78.6±19.0 (cm/s)). HR, PSV, and EDV of the three groups are shown in Table 6.3.

Comparison of A_{cve} and M_{cve} before and after smoking

No significant difference was found in A_{cve} and M_{cve} before and after smoking for heavy smoker group and light smoker group. A'_{cve} significantly increased in heavy smoker group after smoking (Before smoking: 36.7±9.5; after smoking: 41.6±8.0; $p<0.05$). No significant change was found in A'_{cve} for the light smoker group. This is in agreement with previous results of relative change in A_{cve} (Chapter 5). The mean and standard deviation of A_{cve}, M_{cve}, A'_{cve}, and M'_{cve} before and after smoking in heavy smoker group and light smoker group are summarized in Table 6.4.

Comparison of AI and T_{half} between smokers and nonsmokers

Mean AI and T_{half} were significantly different between 10 smokers and 8 nonsmokers ($P<0.05$). AI is significantly higher in 10 smokers, whereas T_{half} was significantly lower in 8 nonsmokers. No significant difference was found in age, BMI, and WEH between two groups. The result is in agreement with that in previous studies [17-18, 23], and suggests that smoking have significant effects on RBC aggregation tendency. AI and T_{half} of two groups were displayed in Fig.6.2 and Fig.6.3 and summarized in Table 6.5.

Table 6.2. Comparison of A_{cve}, M_{cve}, A'_{cve}, and M'_{cve}, among three groups.

	Nonsmokers (n=17)	**Light smokers (n=11)**	**Heavy smokers (n=17)**
A_{cve}	25.1±12.0	26.8±7.7	25.1±12.8
M_{cve}	31.7±11.6	36.2±10.8	28.7±11.4
A'_{cve}	29.3±7.9	35.2±5.1[a]	36.7±9.5[a]
M'_{cve}	36.9±8.6	36.2±10.1	41.5±8.5

A_{cve} =amplitude of cyclic variation in echogenicity; M_{cve}=minimum echogenicity in a cycle; A'_{cve}=compensated A_{cve}; M'_{cve}=compensated A_{cve}; [a]p<0.05.

Table 6.3. HR, PSV and EDV of groups

	Nonsmokers	**Light smokers**	**Heavy smokers**
HR (BPM)	58.0 ± 6.2 (n=17)	64.0±7.7 [a] (n=11)	61.1±8.7 (n=17)
PSV (cm/s)	78.6±19.0 (n=14)	105.1±16.9[a] (n=8)	95.1±16.7 (n=10)
EDV (cm/s)	18.7±5.9 (n=14)	26.6±5.2 (n=8)	21.0±5.6 (n=10)

HR=heart rate; PSV=peak systolic velocity; EDV=end diastolic velocity; [a]p<0.05.

Table 6.4. Mean and Standard deviation of A'_{cve}, M'_{cve} and HR of the heavy smoker group and the light smoker group before and after smoking.

	Light smokers (n=11)		**Heavy smokers (n=17)**	
	Before smoking	**After smoking**	**Before smoking**	**After smoking**
A_{cve}	26.8±7.7	26.3±8.6	25.1±12.8	30.5±11.7
M_{cve}	36.2±10.8	33.8±8.9	28.7±11.4	31.4±13.6
A'_{cve}	35.2±5.1	34.9±6.8	36.7±9.5	41.6±8.0[a]
M'_{cve}	36.2±10.1	38.9±12.8	41.5±8.5	38.9±8.5
HR	64.0±7.7	66.9±6.1	61.1±8.7	64.5±8.9

A_{cve} =amplitude of cyclic variation in echogenicity; M_{cve}=minimum echogenicity in a cycle; A'_{cve}=compensated A_{cve}; M'_{cve}=compensated A_{cve}; ΔHR=increase of HR after smoking; [a]p<0.05.

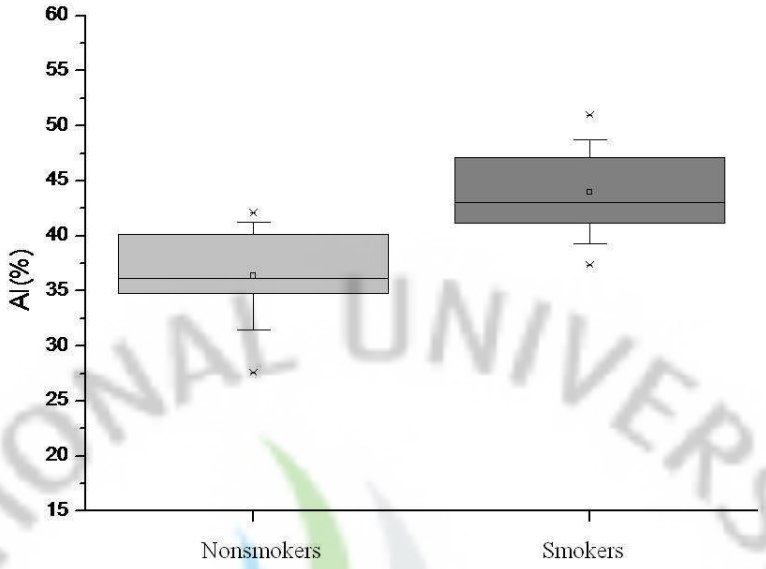

Fig. 6.2. Smoking effects on aggregation index (AI)

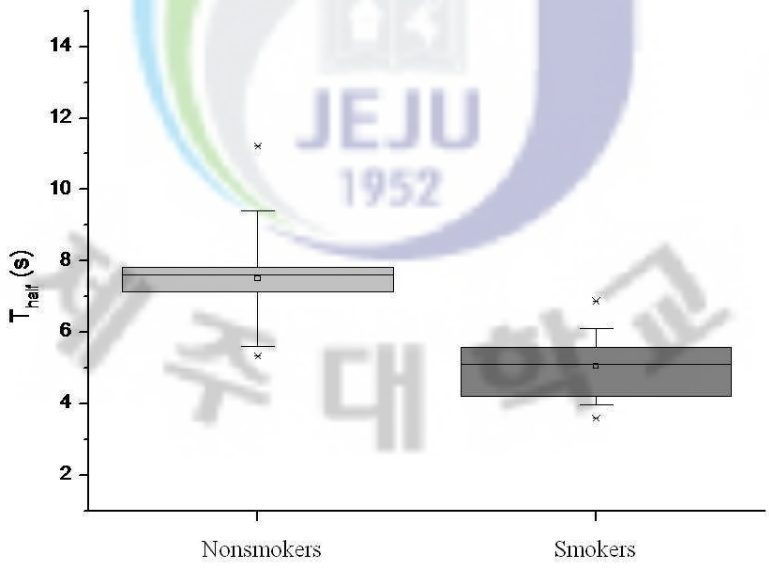

Fig. 6.3 Smoking effects on aggregation index (T_{half})

Table 6.5. Aggregation indicts of smoking group and nonsmoking group

Variable	Category	
	Smoking group (n=10)	Nonsmoking group (n=8)
AI	44.0±4.7	36.3±4.9*
T_{half}	7.5±1.9	5.0±1.1*
DCC	15±4.5	-
SY	6.8±2.8	-
BMI	20.3±1.4	20.5±1.3
Age	25.6±2.6	27.7±2.0
WEH	1.4±0.7	1.2±0.5

6.4 Discussion

Principal findings

The compensated parameter could provide more valuable information. Differences in A'_{cve}, HR, and PSV between smokers and nonsmokers are reported in the present study. The heavy smoker group posted significant increases in A'_{cve}, whereas the light smoker group posted significant increases in HR and PSV. No significant differences in M'_{cve} were present among three groups. Moreover, smoking could acutely increase A'_{cve} in the heavy smoker group, but not in the light smoker group.

The chronic effects of smoking on A'_{cve}

This study demonstrated that smoking had significant chronic effects on A'_{cve} in heavy smokers. Smoking could chronically increase the HR and blood flow velocity. However, increase in these hemodynamic parameters was not in accordance with the increase in A'_{cve},

e.g., the A'_{cve} was highest in heavy smoker group whereas the HR and PSV were highest in light smoker group. Results of *in vitro* experiments [55-56] suggested that the amplitude of CVE may be decreased at high HR or high flow speed. Therefore, the increases of HR and blood flow velocity could not explain the increase in A_{cve}. The increased A'_{cve} in smokers may be explained by the chronic effects of smoking on some hematological parameters, e.g., blood viscosity and RBC aggregation. However, this interpretation should be taken with high caution for the method used to compensate A_{cve} may introduce some variability.

Compensation of tissue attenuation

The effect of tissue attenuation on backscatter power from blood was considered to be related with its depth and compensated by Cloutier [47]. However, BMI was applied to compensate the tissue attenuation in this study. The thickness of tissue may be corrected with BMI. Firstly, BMI was correlated with circumference of waist and calf [94] and consequently BMI may be correlated with the thickness of tissue. Secondly, BMI is defined as the body weight divided by the square of height.

$$\mathrm{BMI}=\frac{\text{mass (kg)}}{(\text{height(m)})^2} \qquad (1)$$

By assuming homogeneous body density

$$\mathrm{BMI}=\frac{\rho(\mathrm{kg/m^3})\mathrm{V(m^3)}}{(\text{height(m)})^2}\propto \rho(\mathrm{kg/m^3})\ \text{thickness(m)} \qquad (2)$$

Based on the derivation of the above formula, BMI may be linearly correlated with the thickness of tissue and thus negatively correlated with the attenuated backscattered power.

Furthermore, it was reported that both calf girth and BMI showed significant correction with broadband ultrasound attenuation ($p<0.01$) [94]. It may explain the linear correlation between A_{cve} and BMI and justify the compensation method used in this study.

Moreover, A'_{cve} significantly increased after smoking in heavy smoker group, but not in the light smoker group. This is in agreement with previous analysis of the relative change of A_{cve} induced by acute smoking with the same smokers (Chapter 5). The relative change of A_{cve} was significantly higher in heavy smoker group compared with the light smoker group. However, no significant results were obtained by the comparing the uncompensated A_{cve}, suggesting that the compensation of A_{cve} may help reduce interference from tissue attenuation and appropriate for comparison among individuals. However, further investigation is required for confirmation.

The potential of A'_{cve} as an index of RBC aggregation

The spatial organization of aggregating red blood cells is considered as the main determinant of the echogenicity of blood [58]. Therefore, the amplitude of CVE may reflect the dynamic range of the variation in RBC aggregation during a cardiac cycle and the minimum echogenicity may present minimum RBC aggregation level.

In this study, no significant differences in M'_{cve} among three groups and in M'_{cve} after smoking were found. The minimum RBC aggregation level was relatively stable. The dynamic range of RBC aggregation was associated with the maximum RBC aggregation level.

Consequently, A'_{cve} may present maximum RBC aggregation level *in vivo*.

6.5 Conclusion

Two hypotheses were proposed in this study: (1) A'_{cve} is significantly higher in smokers compared with nonsmokers. This difference may reflect their different RBC aggregation tendency in essence; (2) M'_{cve} is similar among three groups in this study. The minimum echogenicity in a cardiac cycle may be relatively stable among healthy subjects and A'_{cve} may present maximum RBC aggregation level *in vivo*. However, further studies are still needed to better compensate the effect of tissue attenuation on A_{cve}.

Chapter 7

CONCLUSIONS AND SUGGESTIONS

7.1 Conclusions

The cyclic variation in echogenicity (CVE) was measured from transverse section of the common carotid artery through a GE Voluson e ultrasound system. To explore the origin of this observed CVE, the harmonic echogenicity from porcine blood under steady flow *in vitro* was studied with the same ultrasound system. The harmonic images of aggregating porcine whole blood and non-aggregating RBC suspensions were measured as a function of flow speed under steady flow in a mock flow loop. The harmonic echogenicity of porcine whole blood was significantly higher than the RBC suspension at the same static flow rate. The harmonic echogenicity of porcine whole blood decreased exponentially as flow speed increased from 0 to 40cm/s, whereas the echogenicity of the non-aggregating RBC suspension was not correlated with flow speed. Thus, the shear rate dependent RBC aggregation is a determining factor for the harmonic echogenicity from whole blood and harmonic imaging truly reflects the backscatter from blood and RBC aggregates. However, differences between the blood in common carotid artery *in vivo* and porcine whole blood under the steady flow *in vitro* should be considered. Therefore, further investigation is required.

The cyclic variation in echogenicity from common carotid artery was recorded from 20 nonsmokers and 40 smokers. The acute smoking effects on the observed variation in

echogenicity were studied from 28 smokers. Smoking was proven to acutely change blood echogenicity during a cardiac cycle and that changes in CVE were different for heavy and light smokers. The acute effect of smoking on the hemodynamic parameters could not fully explain the change in CVE. The acute response of RBC aggregation to smoking was suggested as an interpretation. In a further study, the effects of tissue attenuation on A_{cve} were compensated by the Body Mass Index (BMI). The compensated A_{cve} was compared among non-smoker group, light smoker group, and heavy smoker group. A'_{cve} gradually increased from nonsmoker group to light smoker group and to heavy smoker group. A'_{cve} was significantly higher in light smoker group and heavy smoker group compared with the nonsmoking group ($P<0.05$). The difference in A'_{cve} among three groups could not be explained by their different HR and flow speed. RBC aggregation tendency at both low and high shear rate significantly increased from nonsmoker group to light smoker group and to the heavy smoker group. Therefore, differences in A'_{cve} of three groups were suggested to reflect their different RBC aggregation tendency.

On the other hand, M'_{cve} remained stable among three groups, even after smoking. Thus, the minimum RBC aggregation level was relatively constant. Consequently, the dynamic range of the variation in RBC aggregation would present RBC aggregation tendency. This could explain the reason that A'_{cve} could reflect RBC aggregation tendency *in vivo*. Most techniques for the measurement of RBC aggregation are only available for *in vitro* conditions. The current study may help develop a potential index in studying the dynamic changes in red blood cell aggregation *in vivo* using noninvasive ultrasound technology. However, results

from this study have been taken from a limited sample size, so further statistical research is required.

7.2 Suggestions

In this thesis, the increased HR and flow speed were assumed to decrease the amplitude of cyclic variation in echogenicity. This assumption was supported by several *in vitro* experiments. However, this observed cyclic variation in echogenicity was suggested as a result of combined effects from flow shear rate and acceleration. The increased HR and flow speed may increase both shear rate and flow acceleration. Increased shear rate prevents the formation of RBC rouleaux. In contrast, the increased flow acceleration may enhance formation of RBC rouleaux. Therefore, further investigations about the effects of these two hemodynamic parameters on CVE are still required.

BMI was hypothesized to be associated with the thickness of intermediate soft tissue compensating the effects of tissue attenuation on A_{cve} and M_{cve}, but further investigations are required to validate this. To obtain more accurate measurement results, a better compensation method needs to be developed

Smoking has been suggested to acutely increase the RBC aggregation level, especially in heavy smokers. The acute response of smoking to RBC aggregation is still unexplored. This suggestion is expected to be proven by future studies.

BIBLIOGRAPHY

[1] D.-G. Paeng, *et al.*, "Cyclic and Radial Variation of the Echogenicity of Blood in Human Carotid Arteries Observed By Harmonic Imaging," *Ultrasound in Medicine & Biology,* vol. 36, pp. 1118-1124, 2010.

[2] J. F. Stoltz and M. Donner, "Hemorheology: Importance of erythrocyte aggregation," *Clin Hemorheol* pp. 7-15, 1987.

[3] R. R. Puniyani, *et al.*, "Risk factors evaluation in some cardiovascular diseases," *Journal of Biomedical Engineering,* vol. 13, pp. 441-443, 1991.

[4] H. Demiroglu and A. Gurlek, "Altered red blood cell rheology as a predisposing factor for diabetic nephropathy," *Nephron,* vol. 79, pp. 121-2, 1998.

[5] H. Demiroglu, *et al.*, "The effects of age and menopause on erythrocyte aggregation," *Thromb Haemost,* vol. 77, p. 404, Feb 1997.

[6] A. Glacet-Bernard, *et al.*, "Elevated erythrocyte aggregation in patients with central retinal vein occlusion and without conventional risk factors," *Ophthalmology,* vol. 101, pp. 1483-7, Sep 1994.

[7] Y. W. Yuan and K. K. Shung, "Ultrasonic backscatter from flowing whole blood. II: Dependence on frequency and fibrinogen concentration," *The Journal of the Acoustical Society of America,* vol. 84, pp. 1195-1200, 1988.

[8] S. Y. Kim, *et al.*, "Ultrasonic evaluation of erythrocyte aggregation dynamics,"

Biorheology, vol. 26, pp. 723-36, 1989.

[9] Y. W. Yuan and K. K. Shung, "Ultrasonic backscatter from flowing whole blood. I: Dependence on shear rate and hematocrit," *The Journal of the Acoustical Society of America*, vol. 84, pp. 52-58, 1988.

[10] G. Cloutier, *et al.*, "Power Doppler ultrasound evaluation of the shear rate and shear stress dependences of red blood cell aggregation," *IEEE Trans Biomed Eng*, vol. 43, pp. 441-50, May 1996.

[11] D. G. Paeng, *et al.*, "In vivo observation of blood echogenicity variation during a cardiac cycle on human carotid arteries," in *Ultrasonics, 2003 IEEE Symposium on*, 2003, pp. 847-850 Vol.1.

[12] D. Fatkin, *et al.*, "Inhibition of Red Cell Aggregation Prevents Spontaneous Echocardiographic Contrast Formation in Human Blood," *Circulation*, vol. 96, pp. 889-896, August 5, 1997 1997.

[13] *Smoking statistics*. Available: http://www.wpro.who.int/media_centre/fact_sheets/fs_20020528.htm

[14] C. J. L. Murray and A. D. Lopez, "Evidence-Based Health Policy---Lessons from the Global Burden of Disease Study," *Science*, vol. 274, pp. 740-743, November 1, 1996 1996.

[15] E. Ernst, *et al.*, "Blood rheology in healthy cigarette smokers. Results from the MONICA project, Augsburg," *Arteriosclerosis*, vol. 8, pp. 385-8, Jul-Aug 1988.

[16] G. Galea and R. J. Davidson, "Haematological and haemorheological changes associated with cigarette smoking," *J Clin Pathol*, vol. 38, pp. 978-84, Sep 1985.

[17] L. Dintenfass, "Elevation of blood viscosity, aggregation of red cells, haematocrit values and fibrinogen levels with cigarette smokers," *Med J Aust*, vol. 1, pp. 617-20, May 17 1975.

[18] H. Demiroğlu, *et al.*, "Elevated Erythrocyte Aggregation Rates In Smokers: An Impact On The Pathophysiology Of Atherothrombogenesis," *Journal of Medical Research*, vol. 15, pp. 114-7, 1997.

[19] S. M. Shasha, *et al.*, "Red cell filterability in cigarette smokers and its relations to cardiac hypertrophy," *Atherosclerosis*, vol. 98, pp. 91-8, Jan 4 1993.

[20] E. Ernst and A. Matrai, "Abstention from chronic cigarette smoking normalizes blood rheology," *Atherosclerosis*, vol. 64, pp. 75-7, Mar 1987.

[21] L. O. Pilgeram and L. R. Pickart, "Control of fibrinogen biosynthesis: the role of free fatty acid," *J Atheroscler Res*, vol. 8, pp. 155-66, Jan-Feb 1968.

[22] L. O. Pilgeram, "Turnover rate of autologous plasma fibrinogen-14C in subjects with coronary thrombosis," *Thromb Diath Haemorrh*, vol. 20, pp. 31-43, Nov 15 1968.

[23] N. Boss, *et al.*, "[Erythrocyte aggregation in nonsmokers, smokers and myocardial infarct patients]," *Blut*, vol. 27, pp. 191-5, Sep 1973.

[24] S. A. Al-Safi, "Does smoking affect blood pressure and heart rate?," *Eur J Cardiovasc Nurs*, vol. 4, pp. 286-9, Dec 2005.

[25] M. D. Feher, *et al.*, "Acute changes in atherogenic and thrombogenic factors with cessation of smoking," *J R Soc Med*, vol. 83, pp. 146-8, Mar 1990.

[26] B. J. Bain, *et al.*, "Acute changes in haematological parameters on cessation of smoking," *J R Soc Med*, vol. 85, pp. 80-2, Feb 1992.

[27] H. Houben, *et al.*, "Haemodynamic effects of cigarette smoking during chronic selective and non-selective beta-adrenoceptor blockade in patients with hypertension," *Br J Clin Pharmacol*, vol. 12, pp. 67-72, Jul 1981.

[28] G. Grassi, *et al.*, "Mechanisms responsible for sympathetic activation by cigarette smoking in humans," *Circulation*, vol. 90, pp. 248-253, July 1, 1994 1994.

[29] G. D. Lowe, *et al.*, "The effects of age and cigarette-smoking on blood and plasma viscosity in men," *Scott Med J*, vol. 25, pp. 13-7, Jan 1980.

[30] G. Lagrue, *et al.*, "[Red cell filterability, smoking and cardiovascular risk factors (author's transl)]," *Nouv Presse Med*, vol. 8, pp. 4079-81., Dec 24 1979.

[31] K. Salbas, "Effect of acute smoking on red blood cell deformability in healthy young and elderly non-smokers, and effect of verapamil on age- and acute smoking-induced change in red blood cell deformability," *Scand J Clin Lab Invest*, vol. 54, pp. 411-6, Oct 1994.

[32] O. K. Baskurt, *et al.*, "Effect of Superoxide Anions on Red Blood Cell Rheologic Properties," *Free Radical Biology and Medicine*, vol. 24, pp. 102-110, 1998.

[33] W. H. Reinhart and A. Singh, "Erythrocyte aggregation: the roles of cell deformability

and geometry," *European Journal of Clinical Investigation,* vol. 20, pp. 458-462, 1990.

[34] J. Hayano, *et al.*, "Short- and long-term effects of cigarette smoking on heart rate variability," *The American Journal of Cardiology,* vol. 65, pp. 84-88, 1990.

[35] N. Benowitz, "Drug therapy. Pharmacologic aspects of cigarette smoking and nicotine addition," *N Engl J Med,* vol. 319, pp. 1318-1330, November 17, 1988 1988.

[36] D. G. Gilbert, *et al.*, "Effects of smoking/nicotine on anxiety, heart rate, and lateralization of EEG during a stressful movie," *Psychophysiology,* vol. 26, pp. 311-20, May 1989.

[37] A. C. Parrott and G. Winder, "Nicotine chewing gum (2 mg, 4 mg) and cigarette smoking: comparative effects upon vigilance and heart rate," *Psychopharmacology,* vol. 97, pp. 257-261, 1989.

[38] R. P. Sloan, *et al.*, "Effect of mental stress throughout the day on cardiac autonomic control," *Biological Psychology,* vol. 37, pp. 89-99, 1994.

[39] A. Adan and M. Sanchez-Turet, "Influence of smoking and gender on diurnal variations of heart rate reactivity in humans," *Neurosci Lett,* vol. 297, pp. 109-12, Jan 12 2001.

[40] S. C. Peeke and H. V. Peeke, "Attention, memory, and cigarette smoking," *Psychopharmacology (Berl),* vol. 84, pp. 205-16, 1984.

[41] S. V. Stone, *et al.*, "Gender differences in cardiovascular reactivity," *J Behav Med,* vol. 13, pp. 137-56, Apr 1990.

[42] L. V. Fichera and J. L. Andreassi, "Stress and personality as factors in women's

cardiovascular reactivity," *Int J Psychophysiol*, vol. 28, pp. 143-55, Mar 1998.

[43] C. Vogele, "Serum lipid concentrations, hostility and cardiovascular reactions to mental stress," *Int J Psychophysiol*, vol. 28, pp. 167-79, Mar 1998.

[44] R. Seibt, *et al.*, "Cardiovascular reactivity of different mental stress models in normotensives, borderline hypertensives and hypertensives," *Stress Medicine*, vol. 14, pp. 183-193, 1998.

[45]J. Trap-Jensen, "Effects of smoking on the heart and peripheral circulation," *Am Heart J*, vol. 115, pp. 263-7, Jan 1988.

[46] J. Zhang and H. Kesteloot, "Anthropometric, lifestyle and metabolic determinants of resting heart rate. A population study," *European Heart Journal*, vol. 20, pp. 103-110, 1999.

[47] G. Cloutier, *et al.*, "Differences in the erythrocyte aggregation level between veins and arteries of normolipidemic and hyperlipidemic individuals," *Ultrasound in Medicine & Biology*, vol. 23, pp. 1383-1393, 1997.

[48] M. G. M. de Kroon, *et al.*, "Cyclic changes of blood echogenicity in high-frequency ultrasound," *Ultrasound in Medicine & Biology*, vol. 17, pp. 723-728, 1991.

[49] G. Cloutier and K. K. Shung, "Cyclic variation of Doppler backscattering power from porcine blood in a pulsatile flow model," in *Ultrasonics Symposium, 1991. Proceedings., IEEE 1991*, 1991, pp. 1301-1304 vol.2.

[50] G. Cloutier and K. K. Shung, "Study of red cell aggregation in pulsatile flow from

ultrasonic Doppler power measurements," *Biorheology,* vol. 30, pp. 443-61, Sep-Dec 1993.

[51] S. J. Wu and K. K. Shung, "Cyclic variation of Doppler power from whole blood under pulsatile flow," *Ultrasound in Medicine & Biology,* vol. 22, pp. 883-894, 1996.

[52] Y.-H. Lin and K. K. Shung, "Ultrasonic backscattering from porcine whole blood of varying hematocrit and shear rate under pulsatile flow," *Ultrasound in Medicine & Biology,* vol. 25, pp. 1151-1158, 1999.

[53] D.-G. Paeng, *et al.*, "Doppler power variation from porcine blood under steady and pulsatile flow," *Ultrasound in Medicine & Biology,* vol. 27, pp. 1245-1254, 2001.

[54] D. G. Paeng and K. K. Shung, "Cyclic and radial variation of the Doppler power from porcine whole blood," *Ultrasonics, Ferroelectrics and Frequency Control, IEEE Transactions on,* vol. 50, pp. 614-622, 2003.

[55] L. C. Nguyen, *et al.*, "Cyclic Changes in Blood Echogenicity Under Pulsatile Flow Are Frequency Dependent," *Ultrasound in Medicine & Biology,* vol. 34, pp. 664-673, 2008.

[56] C.-C. Huang, "Cyclic Variations of High-Frequency Ultrasonic Backscattering From Blood Under Pulsatile Flow," *Ultrasonics, Ferroelectrics and Frequency Control, IEEE Transactions on,* vol. 56, pp. 1677-1688, 2009.

[57] K.-H. Nam, *et al.*, "Ultrasonic Observation of Blood Disturbance in a Stenosed Tube: Effects of Flow Acceleration and Turbulence Downstream," *Ultrasound in Medicine & Biology,* vol. 34, pp. 114-122, 2008.

[58] G. Cloutier and Z. Qin, "Ultrasound backscattering from non-aggregating and aggregating erythrocytes-a review," *Biorheology*, vol. 34, pp. 443-470, 1997.

[59] K. K. Shung, *et al.*, "Ultrasonic Scattering in Biological Tissues," *The Journal of the Acoustical Society of America*, vol. 94, pp. 3033-3033, 1993.

[60] L. Y. Mo and R. S. Cobbold, "A unified approach to modeling the backscattered Doppler ultrasound from blood," *IEEE Trans Biomed Eng*, vol. 39, pp. 450-61, May 1992.

[61] L. Y. L. Mo and R. S. C. Cobbold, "A Stochastic Model of the Backscattered Doppler Ultrasound from Blood," *Biomedical Engineering, IEEE Transactions on*, vol. BME-33, pp. 20-27, 1986.

[62] J.-S. Lee, *et al.*, "Ga2O3 nanomaterials synthesized from ball-milled GaN powders," *Journal of Crystal Growth*, vol. 244, pp. 287-295, 2002.

[63] L. H. Deng, *et al.*, "Influence of hematocrit on erythrocyte aggregation kinetics for suspensions of red blood cells in autologous plasma," *Biorheology*, vol. 31, pp. 193-205, Mar-Apr 1994.

[64] I. Fontaine, *et al.*, "A System-Based Approach to Modeling the Ultrasound Signal Backscattered by Red Blood Cells," *Biophysical Journal*, vol. 77, pp. 2387-2399, 1999.

[65] *Voluson e ultrasound system* Available: http://www.portableultrasound.com/portable-ultrasound-machines/ge-ultrasound/ge-voluson-i/

[66] *12L-RS Electronic broadband linear array transducer*. Available: http://www.umiultrasound.com/transducers/ge/vivid-s6

[67] *Programs for Digital Signal Processing*. New York: IEEE Press, 1979.

[68] T. X. Missaridis and K. K. Shung, "The effect of hemodynamics, vessel wall compliance and hematocrit on ultrasonic Doppler power: an in vitro study," *Ultrasound in Medicine & Biology,* vol. 25, pp. 549-559, 1999.

[69] M. S. van der Heiden, *et al.*, "Ultrasound backscatter at 30 MHz from human blood: Influence of rouleau size affected by blood modification and shear rate," *Ultrasound in Medicine & Biology,* vol. 21, pp. 817-826, 1995.

[70] D.-G. Paeng, *et al.*, "Echogenicity variations from porcine blood i: the "bright collapsing ring" under pulsatile flow," *Ultrasound in Medicine & Biology,* vol. 30, pp. 45-55, 2004.

[71] P. Tortoli, *et al.*, "Interaction between secondary velocities, flow pulsation and vessel morphology in the common carotid artery," *Ultrasound in Medicine & Biology,* vol. 29, pp. 407-415, 2003.

[72] P. J. Brands, *et al.*, "A noninvasive method to estimate wall shear rate using ultrasound," *Ultrasound in Medicine & Biology,* vol. 21, pp. 171-185, 1995.

[73] Z. Qin, *et al.*, "Kinetics of the "Black Hole" Phenomenon in Ultrasound Backscattering Measurements with Red Blood Cell Aggregation," *Ultrasound in Medicine & Biology,* vol. 24, pp. 245-256, 1998.

[74] D.-G. Paeng, *et al.*, "Investigation of blood under pulsatile flow using ultrasound imaging," *International Congress Series*, vol. 1274, pp. 99-108, 2004.

[75] P. V. C. Hough, "Method and means for recognizing complex patterns," US Patent, 1962.

[76] R. O. Duda and P. E. Hart, "Use of the Hough transformation to detect lines and curves in pictures," *Commun. ACM*, vol. 15, pp. 11-15, 1972.

[77]C. Kimme, *et al.*, "Finding circles by an array of accumulators," *Commun. ACM*, vol. 18, pp. 120-122, 1975.

[78] D. H. Ballard, "Generalizing the Hough transform to detect arbitrary shapes," *Pattern Recognition*, vol. 13, pp. 111-122, 1981.

[79] J. M. Nash, *et al.*, "Dynamic feature extraction via the velocity Hough transform," *Pattern Recognition Letters*, vol. 18, pp. 1035-1047, 1997.

[80] S. Wu, *et al.*, "Non-invasive assessment of arterial distension waveforms using gradient-based Hough transform and power Doppler ultrasound imaging," *Medical and Biological Engineering and Computing*, vol. 39, pp. 627-632, 2001.

[81] S. Golemati, *et al.*, "Using the Hough Transform to Segment Ultrasound Images of Longitudinal and Transverse Sections of the Carotid Artery," *Ultrasound in Medicine & Biology*, vol. 33, pp. 1918-1932, 2007.

[82] P. Soille, "Morphological Image Analysis," P. Soille, Ed., ed: Springer, 1999, pp. 164-165.

[83] T. W. Ridler and S. Calvard, "Picture Thresholding Using an Iterative Selection Method," *Systems, Man and Cybernetics, IEEE Transactions on,* vol. 8, pp. 630-632, 1978.

[84] C. Le Devehat, *et al.*, "Red blood cell aggregation in diabetes mellitus," *Int Angiol,* vol. 9, pp. 11-5, Jan-Mar 1990.

[85] S. Usami, *et al.*, "Microcinephotographic studies on red cell aggregation in steady and oscillatory shear--a note," *Biorheology,* vol. 12, pp. 323-5, Aug 1975.

[86] R. Hahn, *et al.*, "Viscoelasticity and red blood cell aggregation in patients with coronary heart disease," *Angiology,* vol. 40, pp. 914-20, Oct 1989.

[87] T. Chiu, *et al.*, "A robust and scalable clustering algorithm for mixed type attributes in large database environment," in *International Conference on Knowledge Discovery and Data Mining* San Francisco, California, 2001.

[88] G. Mancia, *et al.*, "Smoking impairs baroreflex sensitivity in humans," *Am J Physiol Heart Circ Physiol,* vol. 273, pp. H1555-1560, September 1, 1997 1997.

[89] A. Adan and M. Sánchez-Turet, "Smoking effects on diurnal variations of cardiovascular parameters," *International Journal of Psychophysiology,* vol. 20, pp. 189-198, 1995.

[90] Z. L. Jiang, *et al.*, "Blood flow velocity in the common carotid artery in humans during graded exercise on a treadmill," *Eur J Appl Physiol Occup Physiol,* vol. 70, pp. 234-9, 1995.

[91] U. K. Senturk, *et al.*, "Effect of antioxidant vitamin treatment on the time course of hematological and hemorheological alterations after an exhausting exercise episode in human subjects," *J Appl Physiol*, vol. 98, pp. 1272-1279, April 1, 2005 2005.

[92] E. Varlet-Marie, *et al.*, "Reduction of red blood cell disaggregability during submaximal exercise: Relationship with fibrinogen levels," *Clinical Hemorheology and Microcirculation*, vol. 28, pp. 139-149, 2003.

[93] M. R. Hardeman, *et al.*, "The Laser-assisted Optical Rotational Cell Analyzer (LORCA) as red blood cell aggregometer," *Clin Hemorheol Microcirc*, vol. 25, pp. 1-11, 2001.

[94] A. D. Stewart, *et al.*, "Correcting calf girth discriminates the incidence of falling but not bone mass by broadband ultrasound attenuation in elderly female subjects," *Bone*, vol. 31, pp. 195-198, 2002.